Available online at www.sciencedirect.com

SCIENCE DIRECT®

Biochimica et Biophysica Acta 1752 (2005) 154 – 165

BIOCHIMICA ET BIOPHYSICA ACTA

BBA

http://www.elsevier.com/locate/bba

Complete refolding of bovine β-lactoglobulin requires disulfide bond formation under strict conditions

Makoto Hattori[a,*], Kazuhiko Hiramatsu[a], Takashi Kurata[a], Mika Nishiura[a], Koji Takahashi[a], Akio Ametani[b], Shuichi Kaminogawa[b,1]

[a]*Institute of Symbiotic Science and Technology, Division of Agriscience and Bioscience, Tokyo University of Agriculture and Technology, 3-5-8 Saiwaicho, Fuchu-City, Tokyo 183-8509, Japan*

[b]*Department of Applied Biological Chemistry, The University of Tokyo, Tokyo 113-8657, Japan*

Received 21 May 2005; received in revised form 4 July 2005; accepted 19 July 2005
Available online 9 August 2005

Abstract

β-Lactoglobulin (β-LG) denatured with 6 M guanidine hydrochloride (GdnHCl) containing a reducing agent and subsequently dialysed against phosphate-buffered saline (PBS) resulted in incomplete refolding of this protein despite the fact that the biological activity for retinol-binding was recovered to almost the same degree as that of the native molecule [Hattori, M., Ametani, A., Katakura, Y., Shimizu, M., Kaminogawa, S. J., Biol. Chem. 268 (1993) 22414–22419]. The enzyme probe method, evaluation of hydrophilicity values, in-gel mobility on SDS-PAGE, and evaluation of disulfide bonds with the Ellman method showed exposure of the hydrophobic region(s) and incorrect disulfide bond formation in such dialyzed β-LG molecules. We reveal in this present work that complete refolding could be attained by diluting denatured β-LG with PBS containing a reducing agent, before slow reoxidation of the sulfhydryl groups upon dialysis for gradient removal of the reducing agent in 6 steps. Complete renaturation was confirmed by analyzing the retinol-binding activity, CD spectra, intrinsic fluorescence, binding ability of monoclonal antibodies (mAbs), and SDS-PAGE. Step-by-step disulfide bond formation was considered to be critical for the complete refolding of denatured β-LG. Our method can contribute to establish a procedure for complete refolding of useful recombinant proteins in vitro without such biological aids as chaperones.

Keywords: β-Lactoglobulin; Disulfide bond formation; Refolding

1. Introduction

Unfolding and refolding of proteins have been widely investigated [1] to elucidate the mechanisms for the three-dimensional structure formation of polymer molecules and the maturation of a protein newly synthesized in cells, as well as to produce biologically active recombinant proteins by recombinant DNA technology. Although polypeptide synthesis, structural formation of microdomains, modification of amino acid residues, and assembly of polymers occur in a complicated manner with the biological formation of a protein molecule, the production of biologically active proteins from an aggregated polypeptide in the inclusion bodies of recombinant bacteria requires the refolding of already synthesized polypeptide chains. Refolding processes that can only endow polypeptides with biological activities may not be enough to produce protein pharmaceuticals. Considering the potential for inducing anaphylactic reactions, recombinant proteins as administered pharmaceuticals should have the structurally native form. However, the methods to achieve complete refolding of proteins have not yet been well established. We found in the previous study

Abbreviations: β-LG, β-lactoglobulin; RCM-β-LG, reduced and carboxymethylated β-lactoglobulin; PBS, phosphate-buffered saline; GSH, reduced form of glutathione; GSSG, oxidized form of glutathione; K_{AS}, equilibrium constant; K'_d, dissociation constant; mAb, monoclonal antibody; MES, 2-(*N*-morpholino) ethanesulfonic acid; GdnHCl, guanidine hydrochloride

* Corresponding author. Tel.: +81 42 367 5879; fax: +81 42 360 8830.
E-mail address: makoto@cc.tuat.ac.jp (M. Hattori).
[1] Present address: Nihon University College of Biosource Sciences, 1866 Kamcino, Fujisawa, Kanagawa 252-8510, Japan.

1570-9639/$ - see front matter © 2005 Elsevier B.V. All rights reserved.
doi:10.1016/j.bbapap.2005.07.015

[2] that when bovine β-lactoglobulin (β-LG) was treated with 6 M guanidine hydrochloride containing a reducing agent and subsequently dialysed against PBS, the molecule regained a level of retinol-binding activity similar to that of the native material. However, our panel of monoclonal antibodies could detect structural differences between such renatured and native molecules. Subramaniam et al. [3] have also found that the conformational stability of the renatured β-LG obtained by a method similar to ours was lower than that of native β-LG by evaluating the room-temperature tryptophan phosphorescence.

Bovine β-LG is a globular protein of MW 18,000 as a monomer containing two disulfide bridges as well as a free cysteine residue and can exist as a dimer or tetramer [4]. The structure of β-LG has been widely studied by X-ray crystallography [5–8], NMR [9–11], and other physicochemical methods. This protein consists of nine antiparallel β-sheets and one α-helix to form a calyx-shaped β-barrel structure and is classified as a member of the lipocalin superfamily [12,13]. The physiological function of β-LG is tentatively considered to be the binding and transportation of small hydrophobic ligands such as retinol and fatty acids [14]. Utilizing its structural data and advantage of smallness as a protein molecule, β-LG has also been studied as a model of unfolding [15–18] and refolding [2,10,19–21]. The refolding process of β-LG is unique in that non-native α-helix intermediates appear during an early phase. Elucidation of the β-LG folding mechanism can be used as a model to study the α-helix/β-sheet transition of other proteins such as prion proteins [10,21].

We study in this present work the structural features of β-LG treated for renaturation and develop a new method to achieve complete refolding of β-LG. Many useful proteins that are applicable as pharmaceuticals, including the lipocalin protein family, have a β-barrel structure [22], so the renaturation method we develop in this study can be applied to establish a production procedure for protein pharmaceuticals using recombinant DNA technology.

2. Materials and methods

2.1. Preparation of β-LG and RCM-β-LG

Fresh skim milk from a Holstein cow of the genotype AA for β-LG was supplied by our dairy farm. Crude β-LG was prepared by the method of Armstrong et al. [23] and purified by DEAE-Sephacel (Amersham Pharmacia Biotech, Buckinghamshire, UK) ion-exchange chromatography using linear gradient elution from 0 to 0.5 M of NaCl in a 0.05 M imidazole–HCl buffer (pH 6.7). A single band was obtained for the purified β-LG by PAGE both with and without SDS. RCM-β-LG was prepared by reducing the disulfide bonds in β-LG with 2-mercaptoethanol and then carboxymethylating the free sulfhydryl groups with sodium iodoacetate as described previously [2].

2.2. Preparation and purification of monoclonal antibodies (mAbs)

The ascites fluid containing each mAb was obtained as previously described [2,15,24]. Each mAb was purified with a Bakerbond ABx column (8 ID×250 mm; J. T. Baker, Phillipsburg, NJ, USA) to which each ascites diluted with 4 parts of 10 mM 2-(*N*-morpholino)ethanesulfonic acid (MES) at pH 5.6 was applied. Elution was achieved with a linear gradient from 10 mM MES (pH 5.6) to 250 mM KH_2PO_4 (pH 6.8).

2.3. Denaturation and renaturation of β-LG

β-LG at 2.0 or 0.2 mg/ml was incubated for 3 h at 25 °C in phosphate-buffered saline (PBS; 0.11 M phosphate buffer at pH 7.1 containing 0.04 M NaCl and 0.02% NaN_3) containing 6 M guanidine hydrochloride (GdnHCl) in the presence of 0.14 M 2-mercaptoethanol. The subsequent renaturation treatment was initiated by the procedures summarized in Table 1. A medium bottle (500 ml, Pyrex) with a cap was used in the dialysis step of methods 6–11, and the head space was filled with N_2 gas.

2.4. Measurement of the retinol-binding activity

The retinol-binding activity of β-LG was measured by fluorescence titration [25]. In brief, retinol in ethanol was added to a 2.0 ml solution in a cuvette containing 0.2 or 0.02 mg of protein in PBS. Small increments (5 μl at a time) of the retinol in ethanol at about 100 or 10 μM were added to the cuvette with a micropipette. The mixture was thoroughly mixed and then allowed to equilibrate for 1 min before recording the fluorescence intensity. The fluorescence was measured by a Shimadzu RF-5300PC fluorescence spectrophotometer (Kyoto, Japan) with excitation at 330 nm and emission at 470 nm. The apparent dissociation constant (K'_d) was calculated according to the method of Cogan et al. [26] from the results of fluorescence titration.

2.5. Spectroscopic analyses

CD spectra of 0.1% β-LG in PBS were recorded at 25 °C with a J-720WI automatic recording spectro-polarimeter (JASCO, Tokyo, Japan) in a cell of 1.0 mm path length. The fluorescence intensity of β-LG dissolved in PBS at 0.001% was measured under an excitation wavelength of 283 nm by means of an RF-5300PC fluorescence spectrophotometer (Shimadzu, Kyoto, Japan).

2.6. SDS-PAGE

SDS-PAGE was carried out with 7.5% polyacrylamide according to the method of Weber and Osborn [27]. Protein bands were stained with a Plusone silver staining kit, protein

#9	2.0	6 M GdnHCl+2-ME+EDTA	(I) 10-fold dilution in PBS+1.0 mM GSSG+0.5 mM GSH	0	4 steps to remove GSSG and GSH
			(II) Incubation at 25 °C for 12 h	25	
			(III) Dialysis, (1) 0 M+1.0 mM GSSG+0.5 mM,	4	
			(2) GSH 0 M+1.0 mM GSSG+0.5 mM GSH,		
			(3) 0 M+1.0 mM GSSG+0.5 mM GSH,		
			(4) 0 M+0.75 mM GSSG+0.38 mM GSH,		
			(5) 0 M+0.5 mM GSSG+0.38 mM GSH,		
			(6) 0 M+0.25 mM GSSG+0.125 mM, (7) 0 M, (8) 0 M, (9) 0 M		
#10	2.0	6 M GdnHCl+2-ME+EDTA	(I) 10-fold dilution in PBS+1.0 mM GSSG+0.5 mM GSH	0	5 steps to remove GSSG and GSH
			(II) Incubation at 25 °C for 12 h	25	
			(III) Dialysis, (1) 0 M+1.0 mM GSSG+0.5 mM GSH,	4	
			(2) 0 M+1.0 mM GSSG+0.5 mM GSH,		
			(3) 0 M+1.0 mM GSSG+0.5 mM GSH,		
			(4) 0 M+0.8 mM GSSG+0.4 mM GSH,		
			(5) 0 M+0.6 mM GSSG+0.3 mM GSH,		
			(6) 0 M+0.4 mM GSSG+0.2 mM,		
			(7) 0 M+0.2 mM GSSG+0.1 mM, (8) 0 M, (9) 0 M, (10) 0 M		
#11	2.0	6 M GdnHCl+2-ME+EDTA	(I) 10-fold dilution in PBS+1.0 mM GSSG+0.5 mM GSH	0	6 steps to remove GSSG and GSH
			(II) Incubation at 25 °C for 12 h	25	
			(III) Dialysis, (1) 0 M+1.0 mM GSSG+0.5 mM GSH,	4	
			(2) 0 M+1.0 mM GSSG+0.5 mM GSH,		
			(3) 0 M+1.0 mM GSSG+0.5 mM GSH,		
			(4) 0 M+0.83 mM GSSG+0.42 mM GSH,		
			(5) 0 M+0.67 mM GSSG+0.33 mM GSH,		
			(6) 0 M+0.5 mM GSSG+0.25 mM,		
			(7) 0 M+0.33 mM GSSG+0.17 mM,		
			(8) 0 M+0.17 mM GSSG+0.08 mM, (9) 0 M, (10) 0 M, (11) 0 M		

All reagents were of highest quality commercially available and were solubilized in Milli-Q™ water.
Numbers in parentheses indicate the order of dialysis, and the concentration of GdnHCl in PBS is shown after the number in parentheses.
[a] 2-mercaptoethanol.
[b] PBS containing 6 M GdnHCl, 5 mM 2-ME, and 1 mM Na_2EDTA.
[c] The ratio of denatured β-LG to dialyzing buffer was always 1:100 (5 mL:500 mL). Dialyzing buffer was substituted every 3 h.

(Amersham Pharmacia Biotech, Buckinghamshire, UK), and the stained gels were analyzed by densitometry.

2.7. Enzyme-probe method

The structural difference between native and renatured β-LG was evaluated by the enzyme-probe method [24]. A 320 μl amount of native or treated β-LG (1.25 mg/ml) and 40 μl of α-chymotrypsin (0.2 mg/ml; EC 3.4.21.1, Sigma, St. Louis, MO, USA) in PBS were incubated at 30 °C. At defined times, 40 μl of 2 M HCl was added to the reaction mixture to stop the reaction. The resulting solution was analyzed by reversed-phase HPLC with an ODS-120T column (4.6 IS×250 mm; Tosoh, Tokyo, Japan), and the peak area corresponding to undigested β-LG was measured.

2.8. Competitive enzyme-linked immunosorbent assay (ELISA)

Competitive ELISA with mAbs was carried out as described previously [2]. In brief, the wells of a polystyrene microtitration plate (Maxisorp, Nunc, Roskilde, Denmark) were coated with a β-LG solution. Binding of mAb to β-LG on the solid phase was inhibited by various concentrations of antigens (β-LG, RCM-β-LG, or renatured β-LG) and bound mAb was detected by alkaline phosphatase-labeled goat anti-mouse immunoglobulin (DAKO A/S, Glostrup, Denmark), followed by the substrate reaction of *p*-nitrophenylphosphate. The K_{AS} value between each antigen and mAb was calculated from the results of competitive and noncompetitive ELISA according to the procedure of Hogg et al. [28].

3. Results and discussion

3.1. Structural features of β-LG treated by the various attempts to obtain a renatured form

We evaluated the structural features of β-LG molecules obtained by the renaturation method 1 in Table 1. Although the physiological function of β-LG still remains unclear, β-LG is classified as a member of the lipocalin superfamily and can bind small hydrophobic ligands such as retinol and fatty acids [12]. To investigate changes in the structure of the retinol-binding site in β-LG after the renaturation treatment, fluorescence titration of a mixture of β-LG and retinol was performed to obtain the apparent dissociation constant (K'_d). The K'_d value between renatured β-LG (method 1) and retinol was similar to that between native β-LG and retinol, and the maximum fluorescence intensity, which indicates the maximum amount of bound retinol, was similar between renatured and native β-LG (Fig. 1). Renatured β-LG (method 1) had a similar retinol-binding ability to that of native β-LG. The intrinsic fluorescence and CD spectra were measured to examine the overall protein structure of renatured β-LG (method 1). The spectrum for renatured β-LG (method 1) was similar to that for the native molecule by both methods,

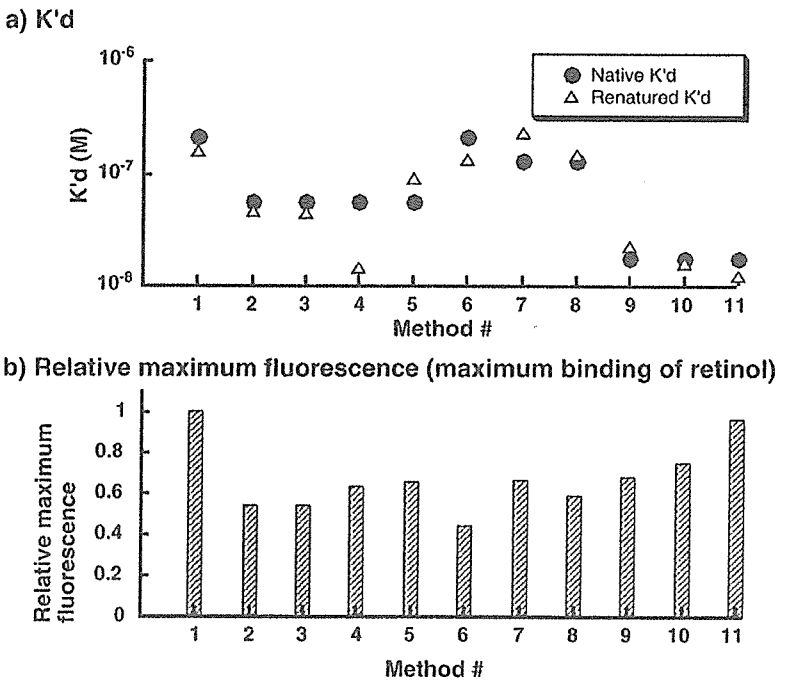

Fig. 1. Retinol-binding activity of renatured β-LG. The retinol-binding activity of native and renatured β-LG was evaluated by fluorescence titration. The apparent dissociation constant (K'_d) was calculated according to the method of Cogan et al. [26] (●) K'_d for β-LG; (△) K'_d for renatured β-LG. (▨) relative maximum fluorescence intensity for renatured β-LG as compared with maximum fluorescence intensity for native β-LG.

indicating that renaturation was virtually complete, as indicated in our previous report (data not shown). Local conformational changes in the renatured β-LG molecules were investigated by competitive ELISA with four anti-β-LG mAbs (21B3, 31A4, 61B4, and 62A6). We have previously shown that these mAbs can detect subtle conformational changes in local areas within a β-LG molecule unfolded or refolded [2,15,24]. The epitopes for mAbs 21B3, 31A4, and 61B4, respectively, contain regions around ^{15}Val-^{29}Ile (β-sheet region), ^{8}Lys-^{19}Trp (short helix and random coil region), and ^{125}Thr-^{135}Lys (α-helix region). The epitope region for mAb 62A6 is close to that for mAb 61B4. A schematic representation of the three-dimensional structure of β-LG and regions containing the epitopes for mAbs is shown in Fig. 2. mAbs 61B4 and 62A6 reacted preferentially to native β-LG, while mAbs 21B3 and 31A4 reacted more strongly to RCM-β-LG (a denatured form of β-LG). mAbs 61B4 and 62A6 showed similar binding affinity to both the native and renatured forms of β-LG (Fig. 3c and d, method 1). The epitope regions for these mAbs are considered to have had a native conformation after the renaturation treatment. However, mAbs 21B3 and 31A4 showed greater affinity to renatured β-LG than to native β-LG (Fig. 3a and b, method 1). The epitope regions for mAbs 21B3 and 31A4 exist in the inner moiety and are not completely exposed on the surface of the β-LG molecule. These regions are considered to have been exposed through denaturation and not to have returned to the inner moiety after the renaturation procedure. These results are consistent with those in our previous report [2]. The epitope region for mAb 21B3 (^{15}Val-^{29}Ile) was found to be the most hydrophobic through the entire sequence of β-LG when the hydrophilicity value was calculated according to the method of Hopp and Woods [29]. The exposure of such a hydrophobic region was experimentally evaluated by the digestibility with chymotrypsin. After 2 h of chymotrypsin digestion, the digestibility of renatured β-LG (method 1) was 45.0%, while that of native β-LG was 21.0%. Renatured β-LG (method 1) was more susceptible to chymotrypsin than was native β-LG. It seems that the hydrophobic regions remained exposed after the renaturation treatment, since chymotrypsin can preferentially digest regions of hydrophobic amino acid residues exposed to the aqueous phase. The number of free thiol groups in native and renatured β-LG (method 1) were, respectively, calculated as 0.977 and 0.601 mol per β-LG molecule by the Ellman method [30]. An SDS-PAGE analysis could show the molecular assembly of native and renatured β-LG. From the results of SDS-PAGE, soluble aggregates were found in renatured β-LG (#1) (Fig. 4 and Table 2, method 1). The results of SDS-PAGE under the non-reducing condition indicated that ~76% of the renatured β-LG molecules were in the monomeric form, while ~17% of the molecule was dimeric, and ~7% was multimeric, assembling more than two polypeptides. On the other hand, soluble aggregates could not be found by SDS-PAGE under

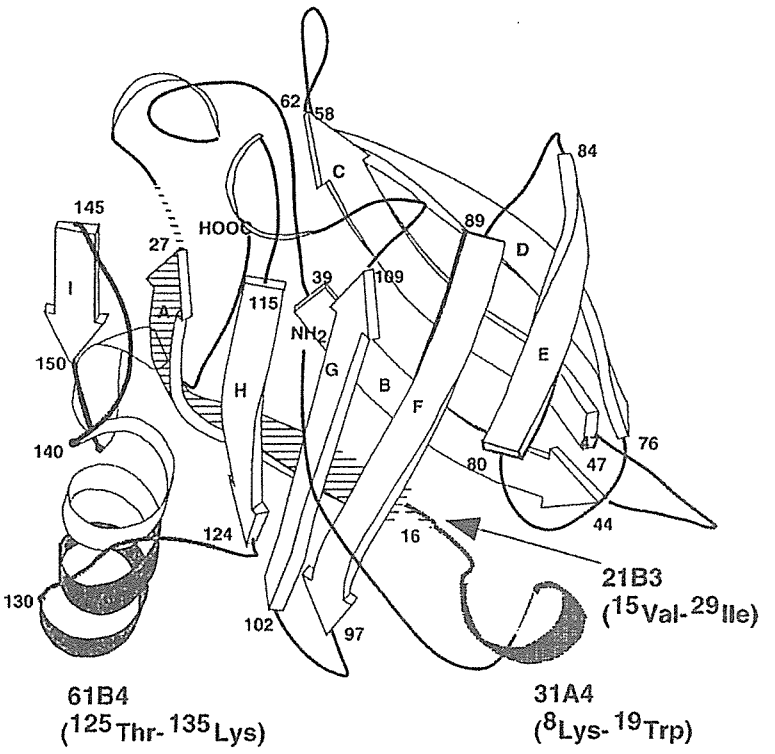

Fig. 2. Schematic representation of the three-dimensional structure of β-LG and regions containing the epitope for mAbs. The epitope for mAbs 21B3, 31A4, and 61B4 contain regions around ^{15}Val-^{29}Ile (β-sheet region), ^{8}Lys-^{19}Trp (short helix and random coil region), and ^{125}Thr-^{135}Lys (α-helix region), respectively. The epitope region for mAb 62A6 is close to that for mAb 61B4.

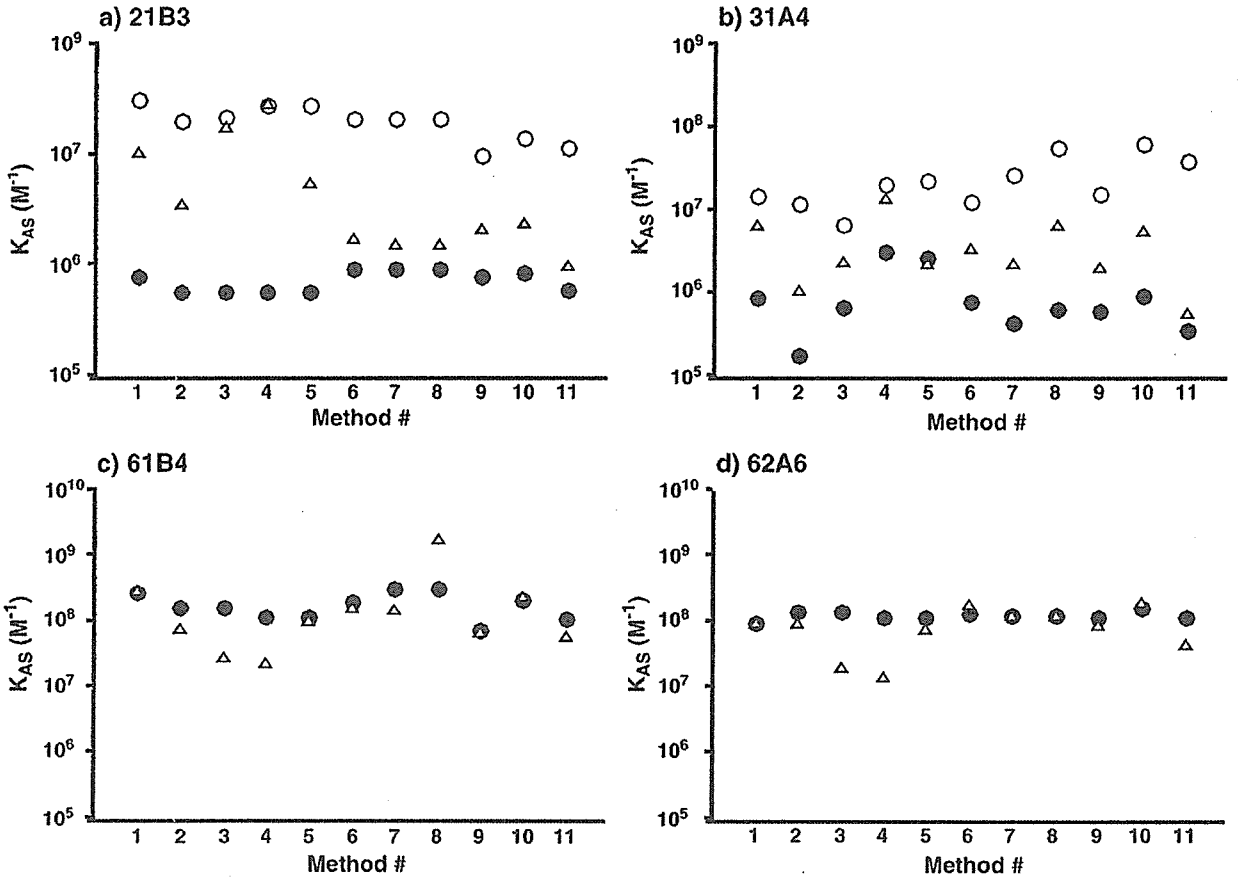

Fig. 3. Equilibrium constants (K_{AS}) of renatured β-LG with mAb. (●) β-LG; (○) RCM-β-LG; (△) renatured β-LG. K_{AS} values were calculated from the results of competitive and noncompetitive ELISA according to the procedure of Hogg et al. [28].

the reduced condition. Differences in the results of SDS-PAGE under the reduced and non-reduced conditions suggest that some of the molecules in the renatured β-LG fraction had been aggregated by intermolecular disulfide bond formation during the treatment. We consider from these results that the β-LG molecules treated by method 1 (Table 1) had hydrophobic surface regions that had failed to be refolded into an internal site and that had incorrectly formed disulfide bond(s). We presume that complete refolding of denatured β-LG would require a decrease in the hydrophobic interaction of the β-LG molecules during the renaturation process under strict control of the formation of disulfide bonds.

3.2. Improvement of the method for renaturing β-LG

First, the protein concentration for dialysis was lowered to 1/10 in order to reduce the intra- and intermolecular interaction (method 2 in Table 1). However, renatured β-LG (method 2) showed similar structural features to those of renatured β-LG (method 1). Although the apparent dissociation constant (K'_d) of renatured β-LG (method 2) with retinol was similar to that of native β-LG, the maximum amount of retinol bound to renatured β-LG (method 2) was lower than that to native β-LG. The difference between the maximum amount of retinol bound to native and to renatured β-LG (method 2) is considered to have resulted from a difference in the structural stability of the retinol-binding site between native and renatured β-LG (method 2). The structural stability of the retinol-binding site in renatured β-LG (method 2) was lower than that in native β-LG. Although complete refolding could not be achieved by method 2, the amount of soluble aggregates was reduced to 6.6%, with all existing only in the dimeric form (Fig. 4 and Table 2).

Dialysis at a low concentration of β-LG was effective for reducing the amount of soluble aggregates, so we then examined the order of removal of the denaturant and reducing agent for the dialysis of a low initial concentration of β-LG (0.2 mg/ml). In our previous study [2], we found that quick removal of the denaturant by dilution or gel filtration led to incomplete refolding of β-LG. Hence, we attempted to achieve renaturation with a slower dialysis process. Method 3 in Table 1 removed the denaturant and reducing agent together; method 4 in Table 1 removed the reducing agent first and then gradually the denaturant; and method 5 in Table 1 removed the denaturant first, and then the reducing agent. Although the K'_d values for renatured β-LGs (methods 3 and 5) for binding to retinol were similar to that for native β-LG, the maximum amount of retinol bound

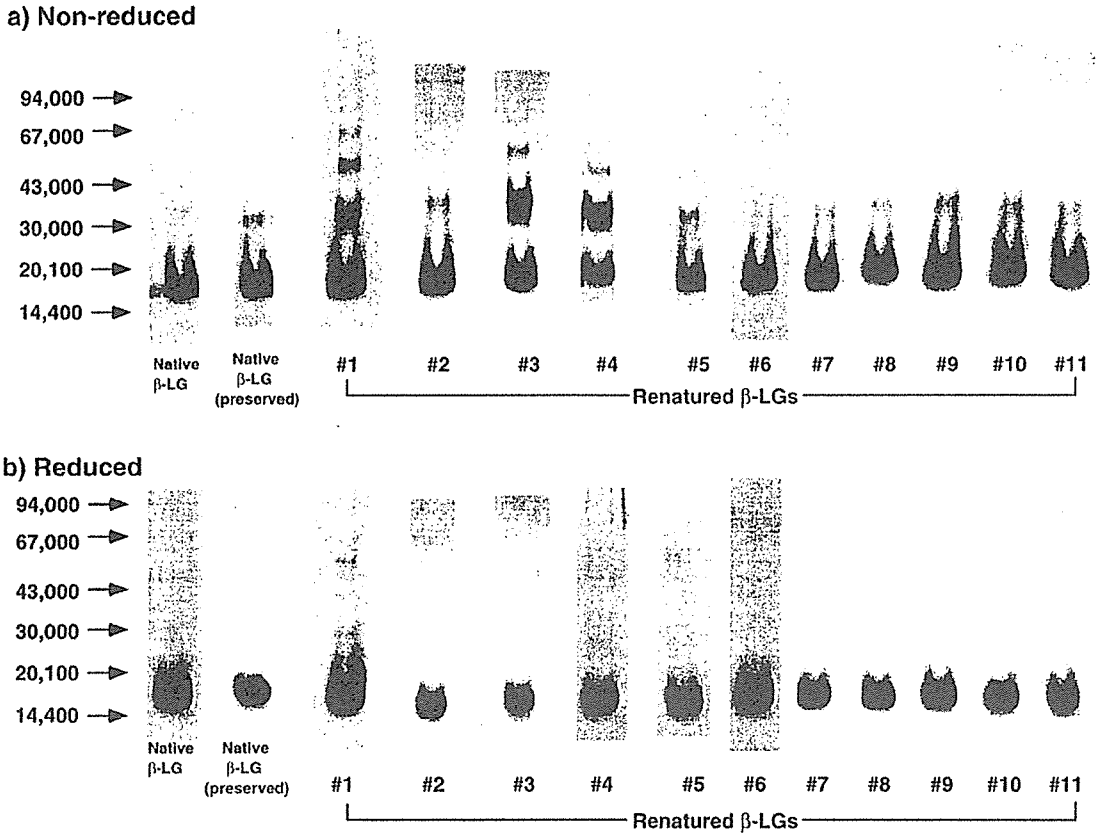

Fig. 4. SDS-PAGE patterns of renatured β-LGs obtained by various renaturation methods. SDS-PAGE was carried out with 7.5% polyacrylamide according to the method of Weber and Osborn [27]. Protein bands were stained with a Plusone silver staining kit, protein (Amersham Pharmacia Biotech). The results were recombined from different gels.

to renatured β-LGs (methods 3, 4, and 5) was lower than that to native β-LG (Fig. 1). It is considered that the structural stability of the retinol-binding sites in β-LG renatured by methods 3, 4, and 5 was lower than that in native β-LG. CD spectra were measured to study the overall structure of β-LGs renatured by methods 3, 4, and 5 (Fig. 5). The results indicated that the wavelength for minimum ellipticity of β-LGs by methods 3 and 4 was blue-shifted (205 nm and 209 nm, respectively) compared with that for native β-LG (216 nm) and that these renatured β-LGs contained a considerable amount of misfolded molecules. Renatured β-LG (method 5) had a similar spectrum to that of native β-LG,

Table 2
Existence ratio of renatured β-LG obtained by different methods evaluated by SDS-PAGE

	Non-reduced condition			Reduced condition		
Method	Monomer	Dimer	>Dimer	Monomer	Dimer	>Dimer
Native (fresh)	98.9	1.1	0	100	0	0
Native (preserved in PBS at 4 °C for 120 h)	96.3	3.7	0	100	0	0
#1	76.2	17.2	6.6	100	0	0
#2	92.5	7.5	0	100	0	0
#3	52.2	43.3	4.5	100	0	0
#4	57.1	35.6	7.3	100	0	0
#5	84.4	14.4	1.2	100	0	0
#6	91.0	9.0	0	100	0	0
#7	97.1	2.9	0	100	0	0
#8	96.4	3.6	0	100	0	0
#9	94.5	5.5	0	100	0	0
#10	97.6	2.4	0	100	0	0
#11	96.2	3.8	0	100	0	0

The existence ratio of renatured β-LG shown in the table indicates the ratio obtained from the results of densitometry after SDS-PAGE.

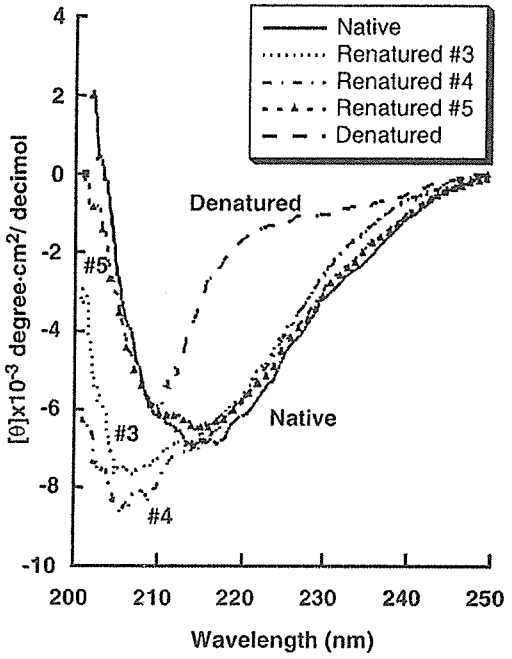

Fig. 5. CD spectra of native and renatured β-LGs in PBS.

indicating that the secondary structure of β-LG renatured by method 5 was similar to that of the native form.

Conformational differences in local areas between native β-LG and renatured β-LGs (methods 3, 4, and 5) were monitored by the binding properties of mAbs (Fig. 3). The structure of the epitope region for mAb 21B3 in β-LGs renatured by methods 3 and 4 was similar to that of a denatured form of β-LG (RCM-β-LG), rather than to that of the native form. The refolding of the epitope regions for mAbs 61B4 and 62A6 in the β-LG molecules renatured by methods 3 and 4 was also found to be incomplete. On the other hand, refolding of the epitope regions for mAbs 61B4 and 62A6 in the β-LG molecules renatured by method 5 was complete, whereas the epitope region for mAb 21B3 was in the intermediate form between native and RCM-β-LG. The results of SDS-PAGE (Fig. 4 and Table 2) show that β-LGs renatured by methods 3 and 4 contained a smaller amount of the monomer (~52% and ~57%, respectively), but a larger amount of soluble aggregates, while ~84% of β-LG renatured by method 5 existed as a monomer. Although complete refolding could not be achieved, method 5 was the most effective among methods 1–5. We consider that removal of the reducing agent after removing the denaturant was more appropriate to establish a method for achieving complete refolding of β-LG.

3.3. Complete refolding of β-LG by controlling the S–S bond formation

To achieve complete refolding of β-LG, strict control of the process for removing the reducing agent was considered to be necessary. Other proteins such as BPTI and hirudin easily denature in the presence of a reducing agent [31,32]. In contrast, β-LG retained a native conformation in the presence of 2-mercaptoethanol as a reducing agent, as indicated by the CD spectral results (data not shown). Burova et al. [33] have also shown that the presence of 2-mercaptoethanol did not affect the secondary structure of β-LG. Our strategy for complete refolding of β-LG was to dilute denatured β-LG with a buffer containing the reducing agent to form the secondary structure, and then to gradually remove the reducing agent to correctly regulate S–S bond formation. Yagi et al. [34] have recently prepared wild-type β-LG and mutants without a free thiol group by recombinant DNA technology in *Pichia pastris*. They showed that intramolecular thiol–disulfide exchange occurred to produce a mixture of molecules with non-native disulfide bonds, and that oligomers were produced by this intermolecular thiol–disulfide exchange in the renaturation process of wild-type β-LG after its denaturation with 8 M urea. In contrast, mutants of β-LG without a free thiol group showed reversible refolding. The strict control of S–S bond formation is considered to have been crucial for complete refolding of β-LG in our study. We employed a mixture of reduced and oxidized glutathione, which are the most commonly used oxido-shuffling reagents, to regulate S–S bond formation in the renaturation of β-LG. Hirose et al. [35], in their study on the renaturation of ovotransferrin from the denatured state, have reported that two-step renaturation was effective to regain the native structure of ovotransferrin without incorrect formation of intramolecular disulfide bonds. In their experiments, denatured protein was incubated at a low temperature (0 °C) in a non-denaturing buffer containing reduced glutathione as the first step, and then reoxidation at a higher temperature (22 °C) in the presence of oxidized glutathione was carried out as the second step. We applied the method of Hirose et al. [35], although with many modifications. Denatured β-LG (2.0 mg/ml) in PBS containing 6 M GdnHCl and 0.14 M 2-mercaptoethanol was 10-fold diluted with PBS containing 0.5 mM GSH and 1 mM GSSG, and the solution was kept at 0 °C for 10 min (Table 1, methods 6–11). The β-LG solution was then incubated for 12 h at 25 °C while gently stirring to slowly reoxidize it. Dilution reduced the GdnHCl concentration to a low level (about 0.6 M) such that it was effective for inhibiting the aggregation of proteins during renaturation [1]. The sample was then dialyzed against a decreasing concentration of the reducing agent at 4 °C to remove the reducing agent rapidly or slowly according to the rate of decrease. The retinol-binding assay, SDS-PAGE analysis, fluorescence measurement, CD spectra measurement, and ELISA with mAbs were then performed to study the structure of β-LGs renatured by methods 6–11. The retinol-binding assay showed that these renatured β-LGs had similar K'_d values to that of

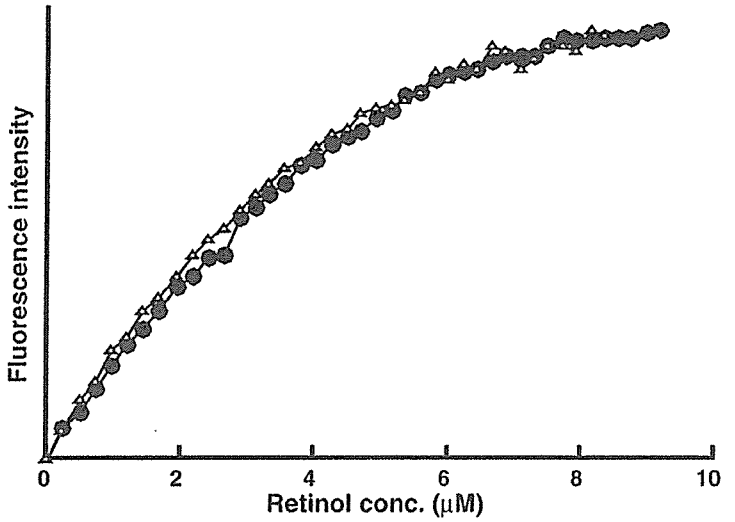

Fig. 6. Retinol-binding activity of renatured β-LG (#11). The retinol-binding activity of native and renatured β-LG (#11) was evaluated by fluorescence titration. (●) native β-LG; (△) renatured β-LG (#11).

the native material (Fig. 1). However, the maximum fluorescence for β-LG by method 6 (the reducing agent was removed in one step) was lower than that for native β-LG (Fig. 1). The maximum florescence for each renatured β-LG approached the value for native β-LG as the number of steps to remove the reducing agent was increased. β-LG renatured by method 11 (6 steps to remove the reducing agent) had the same maximum florescence as that of native β-LG, as shown in Fig. 6. β-LG renatured by method 11 also had a similar CD spectrum to that for native β-LG (Fig. 7a). The result of intrinsic fluorescence measurements showed that native β-LG and β-LG renatured by method 11 had a similar maximum emission wavelength (Fig. 7b). These spectroscopic results indicate that β-LG renatured by method 11 possessed the native global structure. An SDS-PAGE analysis (Fig. 4 and Table 2) revealed that each type of renatured β-LG contained a small amount of soluble aggregate only as a dimer. These results indicate that the renaturation process by methods 6–11 was much more effective than that by methods 1–5. Incorrect formation of disulfide bonds could be suppressed by strictly regulating the reoxidization process (Fig. 4 and Table 2). The dimeric content of each β-LG obtained by

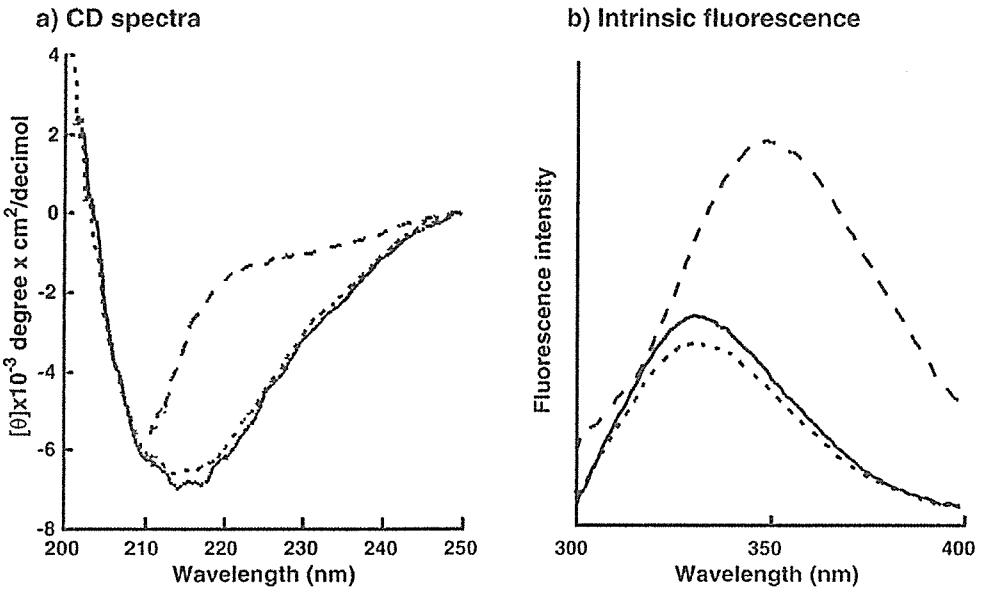

Fig. 7. Spectroscopic analysis of renatured β-LG (#11). (a) CD spectra; (b) intrinsic fluorescence. Native β-LG (—); renatured β-LG (#11) (- - -); denatured β-LG (– – –).

methods 6–11 was similar to that of native β-LG stored at 4 °C for 120 h (3.7%). The binding ability of mAbs indicated that the affinity of all tested mAbs to bind to β-LG renatured by method 11 was similar to that to the native protein (Fig. 3). Hence, we can assume that the local conformation of the epitopes for all four mAbs tested had been renatured by method 11. In conclusion, complete refolding of β-LG could be achieved without using such biological functions as chaperones by first reducing the protein concentration, gradually removing the reducing agent in 6 steps to slowly form the secondary structure, and then gradually removing the reducing agent to correctly regulate S–S bond formation. Useful proteins prepared in bacteria by genetic engineering techniques require three steps after the expression of the proteins in bacteria: (1) inclusion body isolation and washing, (2) solubilization of the aggregated proteins, and (3) renaturation of the solubilized proteins. Although the first two steps can be effectively carried out without difficulty, misfolding and aggregation of the proteins can easily occur in the third step (renaturation), making complete refolding of the proteins very difficult. In addition, many useful proteins include one or more disulfide bonds, and incorrect disulfide bonds can be formed during the renaturation process. The development of effective methods for oxidative protein refolding is very important. The renaturation method reported in this study is valuable for obtaining the active form of useful proteins with a complete native structure by genetic engineering techniques.

References

[1] E. De Bernardez Clark, Protein refolding for industrial processes, Curr. Opin. Biotechnol. 12 (2001) 202–207.

[2] M. Hattori, A. Ametani, Y. Katakura, M. Shimizu, S. Kaminogawa, Unfolding/refolding studies on bovine β-lactoglobulin with monoclonal antibodies as probes. Does a renatured protein completely refold? J. Biol. Chem. 268 (1993) 22414–22419.

[3] V. Subramaniam, D.G. Steel, A. Gafni, In vitro renaturation of bovine β-lactoglobulin A leads to a biologically active but incompletely refolded state, Protein Sci. 5 (1996) 2089–2094.

[4] H.A. McKenzie, β-Lactoglobulins, in: H.A. McKenzie (Ed.), Milk Proteins: Chemistry and Molecular Biology, vol. 2, Academic Press, New York, 1971, pp. 257–330.

[5] M.Z. Papiz, L. Sawyer, E.E. Eliopoulos, A.C.T. North, J.B.C. Findlay, R. Sivaprasadrao, T.A. Jones, M.E. Newcomer, P.J. Kraulis, The structure of β-lactoglobulin and its similarity to plasma retinol-binding protein, Nature 324 (1986) 383–385.

[6] S. Brownlow, C.J. Morais, R. Cooper, D.R. Flower, S.J. Yewdall, I. Polikarpov, A.C. North, L. Sawyer, Bovine β-lactoglobulin at 1.8 Å resolution—Still an enigmatic lipocalin, Structure 5 (1997) 481–495.

[7] B.Y. Qin, M.C. Bewley, L.K. Creamer, H.M. Baker, E.N. Baker, G.B. Jameson, Structural basis of the Tanford transition of bovine β-lactoglobulin, Biochemistry 37 (1998) 14014–14023.

[8] B.Y. Qin, M.C. Bewley, L.K. Creamer, E.N. Baker, G.B. Jameson, Functional implications of structural differences between variants A and B of bovine β-lactoglobulin, Protein Sci. 8 (1999) 75–83.

[9] K. Kuwata, M. Hoshino, V. Forge, S. Era, C.A. Batt, Y. Goto, Solution structure and dynamics of bovine β-lactoglobulin A, Protein Sci. 8 (1999) 2541–2545.

[10] L. Ragona, F. Fogolari, S. Romagnoli, L. Zetta, J.L. Maubois, H. Molinari, Unfolding and refolding of bovine β-lactoglobulin monitored by hydrogen exchange measurements, J. Mol. Biol. 293 (1999) 953–969.

[11] K. Kuwata, R. Shastry, H. Cheng, M. Hoshino, C.A. Batt, Y. Goto, H. Roder, Structural and kinetic characterization of early folding events in β-lactoglobulin, Nat. Struct. Biol. 8 (2001) 151–155.

[12] D.R. Flower, The lipocalin protein family: structure and function, Biochem. J. 318 (1996) 1–14.

[13] L. Sawyer, G. Kontopidis, The core lipocalin, bovine β-lactoglobulin, Biochim. Biophys. Acta 1482 (2000) 136–138.

[14] M.D. Pérez, M. Calvo, Interaction of β-lactoglobulin with retinol and fatty acids and its role as a possible biological function for this protein, J. Dairy Sci. 78 (1995) 978–988.

[15] S. Kaminogawa, M. Shimizu, A. Ametani, M. Hattori, O. Ando, S. Hachimura, Y. Nakamura, M. Totsuka, K. Yamauchi, Monoclonal antibodies as probes for monitoring the denaturation process of bovine β-lactoglobulin, Biochim. Biophys. Acta 998 (1989) 50–56.

[16] A. Laligant, E. Dumay, C.C. Valencia, J.L. Cuq, J.L. Cheftel, Surface hydrophobicity and aggregation of β-lactoglobulin heated near neutral pH, J. Agric. Food Chem. 39 (1994) 2147–2155.

[17] E. Dufour, C. Genot, T. Haertle, β-Lactoglobulin binding properties during its 19 folding changes studied by fluorescence spectroscopy, Biochim. Biophys. Acta 1205 (1994) 105–112.

[18] H. Katou, M. Hoshino, H. Kamikubo, C.A. Batt, Y. Goto, Native-like β-hairpin retained in the cold-denatured state of bovine β-lactoglobulin, J. Mol. Biol. 310 (2001) 471–484.

[19] L.K. Creamer, Effect of sodium dodecyl sulfate and palmitic acid on the equilibrium unfolding of bovine β-lactoglobulin, Biochemistry 34 (1995) 7170–7176.

[20] D. Hamada, S. Segawa, Y. Goto, Non-native α-helical intermediate in the refolding of β-lactoglobulin, a predominantly β-sheet protein, Nat. Struct. Biol. 3 (1996) 868–873.

[21] V. Forge, M. Hoshino, K. Kuwata, M. Arai, K. Kuwajima, C.A. Batt, Y. Goto, Is folding of β-lactoglobulin non-hierarchic? Intermediate with native-like β-sheet and non-native alpha-helix, J. Mol. Biol. 296 (2000) 1039–1051.

[22] D.R. Flower, A.C. North, C.E. Sansom, The lipocalin protein family: structural and sequence overview, Biochim. Biophys. Acta 1482 (2000) 9–24.

[23] J.M. Armstrong, H.A. McKenzie, W.H. Sawyer, On the fractionation of β-lactoglobulin and α-lactalbumin, Biochim. Biophys. Acta 147 (1967) 60–72.

[24] S. Kaminogawa, M. Hattori, O. Ando, J. Kurisaki, K. Yamauchi, Preparation of monoclonal antibody against bovine β-lactoglobulin and its unique affinity, Agric. Biol. Chem. 51 (1987) 797–802.

[25] S. Futterman, J. Heller, The enhancement of fluorescence and decreased susceptibility to enzyme oxidation of retinol complexed with bovine serum albumin, β-lactoglobulin, and the retinol-binding protein of human plasma, J. Biol. Chem. 247 (1972) 5168–5172.

[26] U. Cogan, M. Kopelman, S. Mokady, M. Shintzky, Binding affinities of retinol and related compounds to retinol binding proteins, Eur. J. Biol. Chem. 65 (1976) 71–78.

[27] K. Weber, M. Osborn, The reliability of molecular weight determinations by dodecyl sulfate-polyacrylamide gel electrophoresis, J. Biol. Chem. 244 (1969) 4406–4412.

[28] P.J. Hogg, S.C. Johnson, M.R. Bowles, S.M. Pond, D.J. Winzor, Evaluation of equilibrium constants for antigen-antibody interaction by solid-phase immunoassay: the binding of paraquat to its elicited mouse monoclonal antibody, Mol. Immunol. 24 (1987) 797–801.

[29] T.P. Hopp, K.R. Woods, A computer program for predicting protein antigenic determinants, Mol. Immunol. 20 (1983) 483–489.

[30] G.L. Ellman, Tissue sulfhydryl groups, Arch. Biochem. Biophys. 82 (1959) 70–77.

[31] J.S. Weissman, P.S. Kim, Reexamination of the folding of BPTI: predominance of native intermediates, Science 253 (1991) 1386–1393.
[32] J.Y. Chang, Identification of productive folding intermediates which account for the flow of protein folding pathway, J. Biol. Chem. 268 (1993) 4043–4049.
[33] T.V. Burova, Y. Choiset, V. Tran, T. Haertlé, Role of free Cys121 in stabilization of bovine β-lactoglobulin B, Protein Eng. 11 (1998) 1065–1073.
[34] M. Yagi, K. Sakurai, C. Kalidas, C.A. Batt, Y. Goto, Reversible unfolding of bovine β-lactoglobulin mutants without a free thiol group, J. Biol. Chem. 278 (2003) 47009–47015.
[35] M. Hirose, T. Akuta, N. Takahashi, Renaturation of ovotransferrin under two-step conditions allowing primary folding of the fully reduced form and the subsequent regeneration of the intramolecular disulfides, J. Biol. Chem. 264 (1989) 16867–16872.

Orally Tolerized T Cells Can Form Conjugates with APCs but Are Defective in Immunological Synapse Formation[1]

Wataru Ise,* Kentaro Nakamura,* Nobuko Shimizu,* Hirofumi Goto,* Kenichiro Fujimoto,* Shuichi Kaminogawa,*† and Satoshi Hachimura[2]*

Oral tolerance is systemic immune hyporesponsiveness induced by the oral administration of soluble Ags. Hyporesponsiveness of Ag-specific CD4 T cells is responsible for this phenomenon. However, the molecular mechanisms underlying the hyporesponsive state of these T cells are not fully understood. In the present study, we investigated the ability of orally tolerized T cells to form conjugates with Ag-bearing APCs and to translocate TCR, protein kinase C-θ (PKC-θ), and lipid rafts into the interface between T cells and APCs. Orally tolerized T cells were prepared from the spleens of OVA-fed DO11.10 mice. Interestingly, the orally tolerized T cells did not show any impairment in the formation of conjugates with APCs. The conjugates were formed in a LFA-1-dependent manner. Upon antigenic stimulation, the tolerized T cells could indeed activate Rap1, which is critical for LFA-1 activation and thus cell adhesion. However, orally tolerized T cells showed defects in the translocation of TCR, PKC-θ, and lipid rafts into the interface between T cells and APCs. Translocation of TCR and PKC-θ to lipid raft fractions upon antigenic stimulation was also impaired in the tolerized T cells. Ag-induced activation of Vav, Rac1, and cdc42, which are essential for immunological synapse and raft aggregation, were down-regulated in orally tolerized T cells. These results demonstrate that orally tolerized T cells can respond to specific Ags in terms of conjugate formation but not with appropriate immunological synapse formation. This may account for the hyporesponsive state of orally tolerized T cells. *The Journal of Immunology,* **2005, 175: 829–838.**

Oral tolerance is the state of systemic Ag-specific hyporesponsiveness induced by the oral administration of soluble Ags. The physiological role of oral tolerance is thought to be the prevention of hypersensitivity to food Ags and is a representative form of peripheral tolerance against non-self-Ags under physiological conditions. In addition, a number of experimental autoimmune diseases can be inhibited by oral administration of the corresponding autoantigen (1). Therefore, it is believed that this approach could be used therapeutically to treat autoimmune, inflammatory, and allergic disorders.

Oral tolerance is mediated by T cells. Three mechanisms have been proposed to be involved in the induction of oral tolerance: 1) unresponsiveness of T cells to specific Ags (anergy) (2–4); 2) immune suppression by regulatory T cells that produce TGF-β or IL-10 (5, 6); and 3) the elimination of Ag-specific T cells via apoptosis (clonal deletion) (7). In addition to CD4 T cells, several studies have suggested the role of CD8 T cells (8, 9) or γδ T cells (10, 11) in oral tolerance, especially in terms of their immune suppressive activity. However, CD4 T cells, rather than other T cells, seem to be indispensable to oral tolerance because in vivo depletion of CD4 T cells abrogates oral tolerance induction (12, 13), and CD4 T cells can transfer oral tolerance in vivo (14).

Previous studies demonstrated defects in TCR-mediated signaling in in vivo-tolerized T cells. Upon TCR stimulation, these T cells show incomplete protein tyrosine phosphorylation of signaling molecules (15–17) and impaired nuclear translocation of transcription factors (18–20). We have recently characterized TCR-mediated signaling in orally tolerized T cells. We have used OVA-specific TCR transgenic mice and induced tolerance to peripheral CD4 T cells by the feeding of high doses of OVA. In this experimental system, orally tolerized CD4 T cells show impaired calcium/NFAT signaling upon TCR cross-linking but normal activation of the MAPK pathway (21). Furthermore, we have found that orally tolerized T cells up-regulate caspase activation and show decreased levels of caspase-targeted proteins, such as Grb2-related adaptor downstream of Shc (GADS) and Src homology 2 domain containing leukocyte protein of 76 kDa (SLP-76), which are important adaptor molecules in TCR signaling (22). Thus, it has been suggested that these characteristics of TCR signaling could be responsible for the hyporesponsiveness of orally tolerized T cells.

Most of these studies used artificial stimulation, such as Ab-mediated cross-linking of TCR, to elicit strong signaling and to facilitate biochemical analysis. The events occurring in tolerized T cells upon stimulation with Ag-APCs, which are more physiological ligands for TCR, have not been documented. Upon recognition of specific Ags via TCRs, T cells form conjugates with APCs. The interaction culminates in the formation of a highly organized complex of receptors, adhesion molecules, and intracellular signaling molecules at the interface between the T cells and APCs, the so-called immunological synapse (23). It is well established that upon antigenic stimulation, TCR, protein kinase C-θ (PKC-θ)[3], and LFA-1 polarize to the APC interface and segregate into distinct supramolecular clusters following a precise relative topology (24, 25). This process is mediated, in part, by remodeling of the actin

*Department of Applied Biological Chemistry, University of Tokyo, Tokyo, Japan; and †Department of Food Science and Technology, College of Bioresource Sciences, Nihon University, Kanagawa, Japan

Received for publication June 28, 2004. Accepted for publication April 21, 2005.

The costs of publication of this article were defrayed in part by the payment of page charges. This article must therefore be hereby marked *advertisement* in accordance with 18 U.S.C. Section 1734 solely to indicate this fact.

[1] This work was supported in part by a Grant-in-Aid for Creative Scientific Research (13GS0015) and a Grant-in-Aid for Young Scientists (15780093) from the Ministry of Education, Culture, Sports, Science, and Technology (Japan).

[2] Address correspondence and reprint requests to Dr. S. Hachimura, Department of Applied Biological Chemistry, University of Tokyo, Bunkyo-ku, Tokyo 113-8657, Japan. E-mail address: ahachi@mail.ecc.u-tokyo.ac.jp

[3] Abbreviations used in this paper: PKC-θ, protein kinase C-θ; CTx, cholera toxin B; RBD, rap binding domain; PBD, p21-binding domain; PLC-γ, phospholipase-γ.

0022-1767/05/$02.00

cytoskeleton (26). In addition, lipid rafts containing various signaling molecules are also recruited to the interface and participate in immunological synapse formation (27, 28). Forming a long-lived conjugate and synapse is thought to be required for full T cell activation because the disruption of conjugate and synapse formation, by drug or Ab, results in the inhibition of proliferation and IL-2 production (29). Specific characteristics of immunological synapse formation have been investigated in various cell types, such as Th1, Th2 cells (30), CD8 T cells (31, 32), and immature thymocytes (33, 34). However, it remains unclear whether in vivo-tolerized T cells can form conjugates with APCs and form immunological synapses at the interface.

In this article, we prepared orally tolerized CD4 T cells from OVA-specific DO11.10 mice fed OVA and examined their ability to form conjugates with APCs, to form immunological synapse, and to activate signaling pathways associated with these two events. We demonstrate that orally tolerized T cells can form stable conjugates with Ag-bearing APCs but cannot translocate TCR, PKC-θ, and lipid rafts into the contact site. Biochemical analysis revealed that orally tolerized T cells can activate Rap1, which is required for integrin-mediated adhesion. However, they also showed defects in Ag-induced activation of Vav, Rac, and cdc42, which are critical for immunological synapse formation.

Materials and Methods

Mice

Female BALB/c mice were purchased from CLEA Japan and used at 8–10 wk old. DO11.10 TCR transgenic mice (35) were maintained by backcrossing to BALB/c mice. Female DO11.10 mice were used at 8–12 wk old. All mice used in this study were maintained in the animal facility at the University of Tokyo and used in accordance with the guidelines of the University of Tokyo.

Peptide, Abs, and reagents

OVA323–339 (ISQAVHAAHAEINEAGR) was purchased from Biologica. Rabbit polyclonal anti-Vav, cdc42, Rap1, PKC-θ Ab, and mouse anti-TCR-ζ mAb (6B10.2) were purchased from Santa Cruz Biotechnology. Mouse anti-Rac1 mAb (102), unconjugated or biotin-conjugated rat anti-LFA-1 mAb (M17/4), Cy-chrome-conjugated rat anti-CD4 mAb (H129.19), PE-conjugated rat anti-CD44 (pgp1), and FITC-conjugated streptavidin were purchased from BD Pharmingen. PE-conjugated rat anti-CD62L (MEL14) was purchased from eBioscience. Mouse anti-phosphotyrosine mAb (4G10) was obtained from Upstate Biotechnology. Clonotype-specific mAb KJ1.26 was purified from ascites and conjugated with biotin or FITC in our laboratory. PE-conjugated KJ1.26 was purchased from Caltag Laboratories. Rat anti-MHC class II mAb (M5) was purified and conjugated with FITC in our laboratory. Alexa Fluor-594-conjugated goat anti-rabbit IgG and Alexa Fluor 647-conjugated streptavidin were purchased from Molecular Probes. FITC-conjugated cholera toxin B (CTx) was obtained from Sigma-Aldrich. HRP-conjugated goat anti-rabbit IgG was from Cell Signaling Technology. HRP-conjugate goat anti-mouse IgG was purchased from Amersham Biosciences.

Immunization and oral tolerance induction

For the induction of oral tolerance, OVA (WAKO) was administered to DO11.10 mice in their drinking water (100 mg/ml) for 7 days. The daily intake of OVA was estimated to be ~100 mg/mouse. For immunologic priming, mixture of OVA and CFA was injected i.p. to DO11.10 mice at a OVA dose of 100 μg/mice. The immunized mice were sacrificed 7 days later.

Cell preparation

Splenic CD4 T cells from DO11.10 mice were purified by positive selection using MACS CD4 microbeads (Miltenyi Biotec). The purity of isolated cells was routinely >95%. T cell-depleted splenocytes, such as APCs, were prepared from the spleens of BALB/c mice as described previously (36). APCs used in this study were <5% Thy1.2$^+$.

Proliferation and cytokine secretion assay

Splenic CD4 T cells from DO11.10 mice (1×10^5/well) were cultured with APCs (2×10^5/well) in the presence or absence of various concentrations of OVA323–339 in 96-well flat-bottom plates for indicated periods, and proliferation was assayed by measuring the incorporation of [^{3}H]thymidine (37 kBq/well) during the final 24 h of culture. For cytokine secretion assays, culture supernatants were harvested at the indicated time points. IL-2, IL-4, and IFN-γ concentrations were determined by means of a sandwich ELISA as described previously (36).

Flow cytometric analysis of surface molecules

For analysis of LFA-1 expression, splenic CD4 T cells from DO11.10 mice were stained with biotin-anti-LFA-1, FITC-conjugated streptavidin, PE-KJ1.26, and Cy-chrome-anti-CD4. For analysis of CD62L or CD44 expression, T cells were stained with FITC-KJ1.26, Cy-chrome-anti-CD4, and PE-CD44 or PE-CD62L. Cells were analyzed on a flow cytometer (BD LSR; BD Biosciences) using CellQuest software (BD Biosciences).

In vivo OVA-specific Ab production

DO11.10 mice were immunized i.p. with 100 μg of OVA in the form of an emulsion in CFA. Seven days after, the mice were boosted with 100 μg of OVA emulsified in IFA. Seven days after the boosting, the mice were bled, and OVA-specific IgG titer of their sera was measured by ELISA as described previously (37).

T-APC conjugate formation assay

APCs (2×10^5/well) were pulsed with the indicated concentrations of OVA323–339 for 2 h in 96-well round-bottom plates. Splenic CD4 T cells from DO11.10 mice were mixed with APCs at a 1:1 ratio and centrifuged briefly. After incubation for the indicated period at 37°C, cells were vigorously pipetted to disrupt nonspecific conjugates. Cells were then fixed with 2% paraformaldehyde for 10 min at room temperature. Cells were stained with FITC-anti-MHC class II, PE-KJ1.26, and Cy-chrome-anti-CD4 Abs and analyzed by flow cytometry. Conjugates were determined as the percentage of CD4$^+$KJ1.26$^+$ events that were also MHC class II$^+$.

Confocal microscopy

Splenic CD4 T cells (5×10^5) from DO11.10 mice were mixed with APCs (5×10^5), which had been previously pulsed with 20 μM OVA323–339 for 2–4 h, and incubated at 37°C for 30 min. For lipid raft staining, CD4 T cells were stained with FITC-CTx before incubation with APCs. Cells were then fixed with 4% paraformaldehyde in PBS for 10 min. In the case of PKC-θ staining, cells were permeabilized with 0.1% Triton X-100 in PBS for 2 min. Cells were blocked overnight with 1% BSA/PBS and stained with biotin-KJ1.26 followed by Alexa Fluor 647-streptavidin. For PKC-θ staining, cells were further stained with rabbit anti-PKC-θ followed by Alexa Fluor 594-conjugated anti-rabbit IgG. Staining was performed for 1 h each. All images were taken using a Fluoview FV500 laser scanning confocal microscope (Olympus).

Pull-down assay, immunoprecipitation, and immunoblot

APCs were pulsed with 20 μM OVA323–339 for 4 h at 37°C, after which they were washed three times. APCs were then fixed with 0.2% paraformaldehyde for 10 min to avoid activation of signaling molecules. Splenic CD4 T cells (3×10^6) from DO11.10 mice were mixed with peptide-pulsed APCs (3×10^6) for the indicated times at 37°C. Reactions were stopped by the addition of ice-cold PBS.

For analysis of Rap1, cells were lysed in 25 mM Tris (pH 7.5), 250 mM NaCl, 1.25 mM $MgCl_2$, 10% glycerol, 0.5% Nonidet P-40, and a mixture of protease inhibitor (Roche). Cell nuclei were removed by centrifugation. Clarified lysates were incubated with GST-fusion, Ral GDS-rap binding domain (RBD) (Upstate Biotechnology) at 4°C for 1 h. The GST-Ral GDS-RBD-bound proteins were washed and analyzed by SDS-PAGE. After electrophoresis, the proteins were transferred onto polyvinylidene difluoride membranes for immunoblotting. Blots were probed with rabbit anti-Rap1 followed by HRP-conjugated anti-rabbit IgG. The immunoblots were developed by ECL (Amersham Biosciences). In addition, 10% of whole cell lysates from each sample was run to assess the total amount of Rap1 present. For analysis of Rac1 and cdc42 activation, cells were lysed in 25 mM HEPES (pH 7.5), 150 mM NaCl, 1% legpal CA-630, 10 mM $MgCl_2$, 1 mM EDTA, 10% glycerol, and a mixture of protease inhibitor. Cell lysates were incubated with GST-fusion, PAK-1 p21-binding domain (PBD) (Upstate Biotechnology) at 4°C for 1 h. The GST-PAK-1 PBD-bound proteins were analyzed as described above. Blots were probed with mouse anti-Rac1 or rabbit anti-cdc42 followed by HRP-conjugated

anti-mouse IgG or HRP-conjugated anti-rabbit IgG, respectively. The total amount of Rac1 or cdc42 in the cell lysates was determined as described above.

To analyze tyrosine phosphorylation of Vav, cells were lysed in 20 mM Tris (pH 7.5), 150 mM NaCl, 5 mM EDTA, 1% Nonidet P-40, 1 mM Na_3VO_4, 50 mM NaF, 10 mM Na_2MnO_4, and a mixture of protease inhibitor. Cell extracts were incubated with protein G-Sepharose conjugated with rabbit anti-Vav. The precipitates were subjected to immunoblotting as described above, using anti-phosphotyrosine mAb 4G10 followed by HRP-conjugated anti-mouse IgG. The amount of Vav protein was determined by stripping the phosphotyrosine blot and reprobing with rabbit anti-Vav followed by HRP-conjugated anti-rabbit IgG.

Biochemical isolation of lipid raft fraction

APCs were pulsed with 50 μM OVA323–339 for 4 h at 37°C, after which they were washed three times. Splenic CD4 T cells (3×10^7) from DO11.10 mice were mixed with peptide-pulsed APCs (3×10^7) for the indicated times at 37°C. The reaction was stopped by adding ice-cold PBS. Cells were then lysed with 1 ml of lysis buffer containing 25 mM Tris (pH 7.5), 150 mM NaCl, 5 mM EDTA, 1% Brij 98, 50 mM NaF, 1 mM Na_3VO_4, 10 mM Na_2MnO_4, and a mixture of protease inhibitor. The lysates were homogenized with 20 strokes of a Dounce homogenizer and centrifuged. Supernatants were collected and mixed with an equal volume of 80% sucrose solution and overlaid with 6.5 ml of 30% sucrose and 3.5 ml of 5% sucrose solution. The samples were subjected to ultracentrifugation in a Hitachi RPS40T rotor (Hitachi) at 35,000 rpm at 4°C for 16 h. Twelve fractions were collected from the top of the gradient. Fractions containing lipid rafts were determined using HRP-conjugated CTx. Fractions 3 and 4 or fractions 10–12 were combined and referred to as raft fractions or nonraft fractions, respectively. Proteins in raft fractions were concentrated by acetone precipitation. Pooled raft and nonraft fractions were subjected to SDS-PAGE and Western blotting with mouse anti-TCR-ζ or rabbit anti-PKC-θ, followed by HRP-conjugated anti-mouse IgG or HRP-conjugated anti-rabbit-IgG, respectively.

Statistical analyses

Statistical significance was assessed by Student's t test, with significance accepted at the $p < 0.05$ level.

Results

Induction of oral tolerance in DO11.10 mice

To obtain orally tolerized T cells, OVA was administered to DO11.10 TCR transgenic mice in their drinking water for 7 days. CD4 T cells were isolated from the spleens of these mice or control DO11.10 mice, which had been administered OVA-free water. First, we checked the expression levels of clonotype TCRs and naive/memory markers on CD4 T cells from OVA-fed mice. As shown in Fig. 1*A*, expression of KJ1.26$^+$ TCR was slightly down-regulated in CD4 T cells from OVA-fed mice. However, significant levels of KJ1.26$^+$ TCR were expressed on these CD4 T cells. In addition, the percentage of KJ1.26$^+$ T cells in CD4 T cells in OVA-fed mice was almost the same compared with that observed in control mice. Analysis of CD62L and CD44 expression revealed that ~60–70% of KJ1.26$^+$ T cells showed phenotype of previously primed T cells. Therefore, it seems that oral administration of OVA to DO11.10 was effective to prime Ag-specific T cells.

Next, the functional response of splenic CD4 T cells from these mice was analyzed by measuring both proliferation and IL-2 production upon stimulation with OVA323–339 and APCs at several time points. As shown in Fig. 1, *B* and *C*, both the proliferative response and IL-2 production were significantly decreased in CD4 T cells from OVA-fed DO11.10 mice at any time point of the culture. Furthermore, in vivo OVA-specific Ab response elicited by OVA immunization in OVA-fed mice was examined. Compared with non-OVA fed control mice, anti-OVA IgG response was significantly reduced in OVA-fed mice (Fig. 1*D*). Consequently, we concluded that oral administration of OVA successfully induced systemic tolerance and hyporesponsiveness of Ag-specific CD4 T cells in DO11.10 mice. Hereafter, we designate CD4 T cells from non-OVA fed or OVA-fed DO11.10 mice as untreated control or orally tolerized T cells, respectively.

Orally tolerized T cells can form stable conjugates with APCs

Efficient TCR signaling following T cell activation requires conjugate formation with an APC (38). The hyporesponsive state of orally tolerized T cells may be due to inefficient conjugate formation. We first asked whether orally tolerized DO11.10 T cells could form stable conjugates with OVA-bearing APCs. T cell-depleted splenocytes from BALB/c mice were pulsed with OVA323–339 and incubated with DO11.10-splenic CD4 T cells. T cell-APC conjugates were measured using flow cytometry by staining with KJ1.26 and anti-MHC class II mAb. Interestingly, we found that orally tolerized T cells have no impairment in their formation of conjugates with APCs. Within 30 min of incubation, orally tolerized T cells formed conjugates with APCs pulsed with 1 μM OVA323–339, at comparable levels with untreated control T cells (Fig. 2*A*). Next, we checked the kinetics and Ag dose response of conjugate formation. In this system, conjugate formation occurred rapidly, within minutes of mixing, and reached maximal conjugation at ~30 min (Fig. 2*B*). Orally tolerized T cells formed conjugates more efficiently than untreated control T cells after 5 and 15 min of incubation (Fig. 2*B*). However, comparable levels of conjugate formation were seen between these T cells after 30 min. The conjugates formed by these T cells were stable for at least 3 h (data not shown). Conjugate formation was completely Ag dose dependent, and no difference in Ag dose dependency was seen between untreated control and orally tolerized T cells (Fig. 2*C*). These results clearly show that orally tolerized T cells can respond to specific Ags quite normally in terms of forming APC conjugates.

TCR-mediated recognition of peptide/MHC complexes on APCs triggers inside-out signaling, leading to integrin activation and integrin-mediated formation of T-APC conjugates. Among a number of molecules, the β_2-integrin LFA-1 plays an important role in conjugate formation (39). Therefore, LFA-1 expression on the surface of these T cells was analyzed by FACS. Orally tolerized T cells expressed slightly higher levels of LFA-1 than untreated control T cells (Fig. 3*A*); however, this difference had no effect on the efficiency of conjugate formation (Fig. 2). The addition of anti-LFA1 mAb to the cultures completely blocked conjugate formation by both untreated control and orally tolerized T cells (Fig. 3*B*). These results show that orally tolerized T cells form conjugates with APCs in a LFA-1-dependent manner.

The small GTPase, Rap1, is a signaling molecule that plays a pivotal role in mediating inside-out signals to activating integrins (40). Rap1 activation by TCR stimulation enhances the adhesive activity of LFA-1 and, thus, regulates LFA-1/ICAM-1-mediated interactions between T cells and APCs (41, 42). Because orally tolerized T cells could form stable conjugates with APCs in a LFA-1-dependent manner, we thought that signaling pathways, leading to Rap1 activation, should be intact in orally tolerized T cells. We examined Ag-induced Rap1 activation in T cells by a pull-down assay using GST-RalGDS-RBD, which binds specifically to Rap1-GTP (43). As shown in Fig. 3*C*, antigenic stimulation significantly induced Rap1 activation in orally tolerized T cells. Rap1 activation in tolerized T cells was evident 5 min after stimulation and persisted for as long as 30 min. The levels of active Rap1 were slightly higher in orally tolerized T cells than in untreated control T cells. Thus, it was suggested that Rap1-mediated activation of LFA-1 could occur normally in orally tolerized T cells upon antigenic stimulation, resulting in efficient formation of conjugates with APCs.

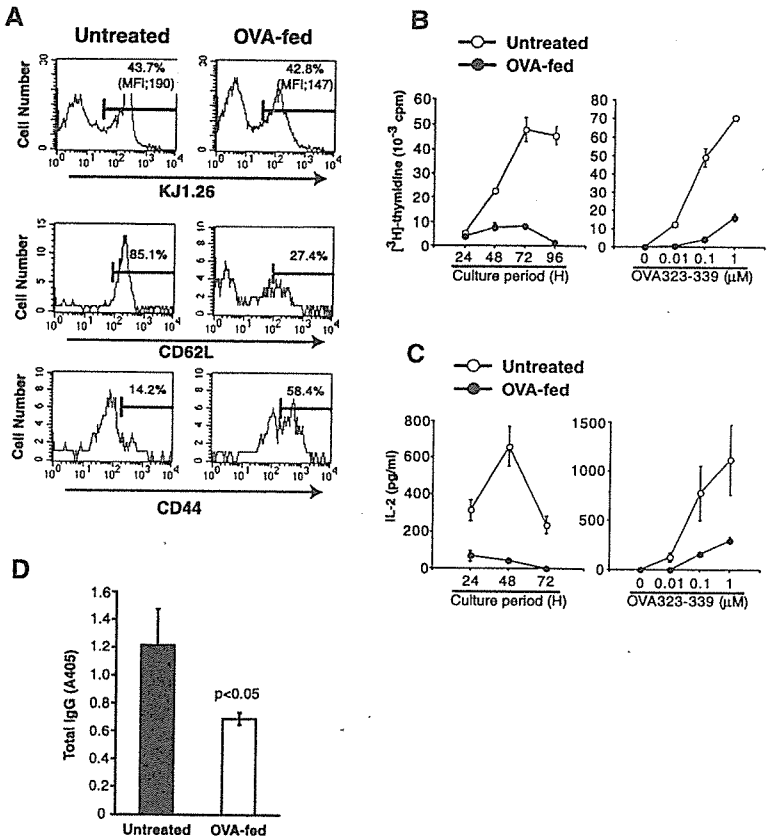

FIGURE 1. Oral tolerance induction in DO11.10 mice. *A*, Splenic CD4 T cells from untreated control or OVA-fed DO11.10 mice were stained with clonotype-specific mAb KJ1.26. Mean fluorescence intensity (MFI) of KJ126$^+$ TCR and percentages of KJ1.26$^+$ T cells in total CD4 T cells are indicated. CD4 T cells were also stained with KJ1.26 and anti-CD62L or anti-CD44 mAb. Expression of CD62L and CD44 on KJ1.26$^+$CD4 T cells are shown. Percentages of CD62L^{high} and CD44^{high} T cells in KJ1.26$^+$CD4 T cells are indicated. *B*, Splenic CD4 T cells from untreated control (○) or OVA-fed DO11.10 mice (●) were stimulated with 0.1 μM OVA323–339 plus APCs for the indicated periods (*left*) or stimulated with indicated concentration of OVA323–339 plus APCs for 72 h (*right*). Proliferation was measured by [^{3}H]thymidine uptake. The data are shown as the average of triplicate cultures ± SD. The results shown are representative of more than three independent experiments. *C*, Splenic CD4 T cells from untreated control (○) or OVA-fed DO11.10 mice (●) were stimulated with 0.1 μM OVA323–339 plus APCs for the indicated periods (*left*) or stimulated with indicated concentration of OVA323–339 plus APCs for 48 h (*right*). IL-2 concentration in the culture supernatants was determined by ELISA. The data are shown as the average of triplicate cultures ± SD. The results shown are representative of more than three independent experiments. *D*, Untreated control or OVA-fed DO11.10 mice were immunized i.p. with OVA/CFA. Seven days later, the mice were boosted i.p. with OVA/IFA. The anti-OVA total IgG titer of sera collected 7 days after boosting was measured by ELISA. The data represent five mice per group and are shown as the average ± SD. Similar results were obtained in one further experiment.

Translocation of TCR, PKC-θ, and lipid rafts into the T cell-APC contact site is defective in orally tolerized T cells

It has been shown that T cells interacting with APCs accumulate Ag receptors, coreceptors, and adhesion and signaling molecules at the site of cell-cell contact, which is called the immunological synapse (23, 44). Formation of the immunological synapse is thought to be required for full activation of T cells, such as their proliferation and IL-2 production (29). We next examined whether orally tolerized T cells could accumulate signaling molecules to the contact site with APCs. Confocal microscopy was performed to investigate localization of TCR (KJ1.26$^+$ TCR) and PKC-θ at the interface between T cells and Ag-bearing APCs. T cells were mixed with APCs for 30 min because conjugate formation was predetermined optimal at this time point (Fig. 2). Fig. 4*A* shows a representative set of images of TCR and PKC-θ localization in both untreated control and orally tolerized T cells conjugated to peptide-pulsed APCs. We counted the number of KJ1.26$^+$T cell-APC conjugates with translocation of TCR and PKC-θ to the contact site. Fig. 4*B* shows the frequencies of KJ1.26$^+$ T cell-APC conjugates with polarized TCR or PKC-θ. The frequency of conjugates with polarized TCR was 52.5% in untreated control T cells but was 25% in orally tolerized T cells. PKC-θ analysis showed similar results. The frequency of conjugates with polarized PKC-θ was 52.6% in untreated control T cells but was only 20% in orally tolerized T cells. These differences were statistically significant ($p < 0.001$ for TCR and $p < 0.01$ for PKC-θ). Importantly, the results indicate that immunological synapse formation was impaired in orally tolerized T cells.

It has been demonstrated that lipid rafts function as platforms for the assembly of signaling complexes and play an important role in T cell signaling (27, 45, 46). Upon antigenic stimulation, lipid rafts on T cells recruit signaling molecules and move to the contact site with APCs. To determine whether lipid raft signaling functions normally in orally tolerized T cells, we first examined lipid raft polarization to the interface between T cells and Ag-bearing APCs. Lipid rafts can be visualized by confocal microscopy with the use of fluorescently labeled CTx subunits. CTx specifically binds to the glycosphingolipid GM1, which is enriched in membrane lipid rafts (47). As can be seen in Fig. 5*A*, stimulation of untreated control T cells with Ag-pulsed APCs for 30 min induced translocation of lipid rafts to their contact area. However, the majority of orally tolerized T cells expressed their lipid rafts around the

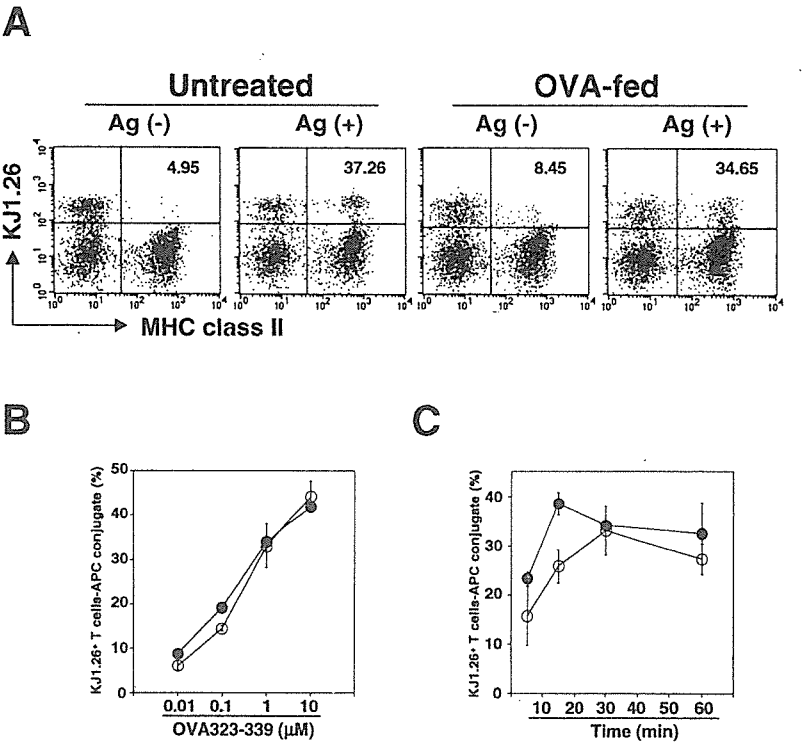

FIGURE 2. Conjugate formation of orally tolerized T cells with Ag-bearing APCs. Splenic CD4 T cells from untreated control or OVA-fed DO11.10 mice were mixed with APCs prepulsed with 1 μM OVA323–339. After 30 min, cells were harvested, fixed, and stained with anti-CD4, KJ1.26, and anti-MHC class II. A representative staining profile with KJ1.26 and anti-MHC class II mAb, and the percentage of double positive cells are shown. *B* and *C*, APCs were prepulsed with 0.01–10 μM (*B*) or 1 μM (*C*) OVA323–339 and mixed with splenic CD4 T cells from untreated control (○) or OVA-fed (●) DO11.10 mice for 30 min (*B*) or 5, 15, 30, and 60 min (*C*). The percentages of MHC class II$^+$ cells within CD4$^+$ KJ1.26$^+$ T cell population were determined. The results are shown as the average from triplicate cultures ± SD. The results are representative of three independent experiments.

plasma membrane, even if they formed conjugates with APCs. The frequency of KJ1.26$^+$ T cell-APC conjugates with polarized lipid rafts was 63.2% in untreated control T cells but 22% in orally tolerized T cells. We next investigated whether signaling molecules translocate to the lipid rafts. To prepare the detergent insoluble raft fractions, cell lysates were ultracentrifuged over a sucrose step-gradient. The positions of raft and nonraft fractions in the gradient were revealed by reactivity with CTx (data not shown). Upon antigenic stimulation, small but readily detectable increases in the amount of TCR-ζ and PKC-θ were seen in the lipid raft fractions in untreated control T cells (Fig. 5*B*). As expected, TCR-ζ and PKC-θ were barely detectable in lipid raft fractions in orally tolerized T cells upon stimulation with Ag (Fig. 5*B*). These results indicate that orally tolerized T cells have defects in their polarization of lipid rafts and translocation of signaling molecules into lipid rafts upon antigenic stimulation.

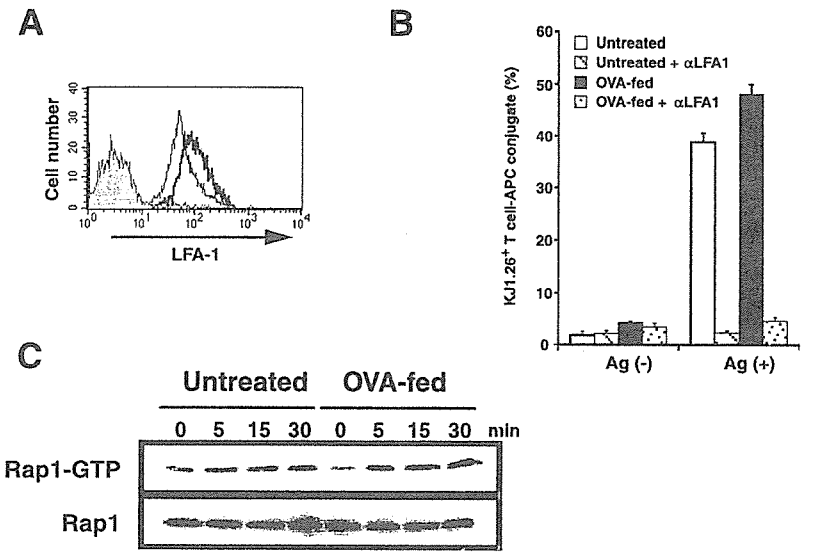

FIGURE 3. LFA-1-dependent conjugate formation by orally tolerized T cells. *A*, The expression levels of LFA-1 on the surface of CD4KJ1.26 cells from untreated control (thin line) or OVA-fed (thick line) DO11.10 mice were determined by FACS. The data is a representative of three independent experiments. *B*, APCs were prepulsed with 1 μM OVA323–339 and mixed with splenic T cells from untreated control or OVA-fed DO11.10 mice for 30 min, in the presence or absence of anti-LFA-1 mAb. The percentages of MHC class II$^+$ cells within the CD4$^+$KJ1.26$^+$ T cell population were determined. The results are shown as the average from triplicate cultures ± SD. The data are representative of three independent experiments. *C*, Splenic CD4 T cells were incubated for the indicated times with APCs prepulsed with 20 μM OVA323–339. Cells were lysed, and active GTP-bound Rap1 was detected with a pull-down assay using GST-fusion Ral GDS-RBD. Bound Rap1 (*upper panels*) and total Rap1 (*lower panels*) were detected by Western blotting with anti-Rap1 Ab.

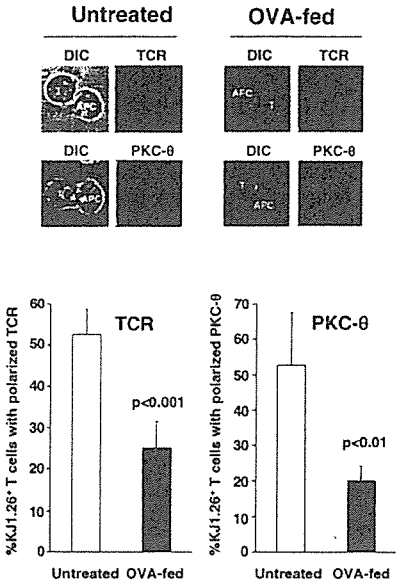

FIGURE 4. Ag-induced translocation of TCR and PKC-θ to the contact site in orally tolerized T cells. Splenic CD4 T cells were incubated with APCs prepulsed with 1 μM OVA323–339. After 30 min, cells were fixed, permeabilized, and stained for KJ1.26$^+$TCR and PKC-θ for confocal microscopy. In the *upper panels*, representative images for T-APC conjugates and the localization of TCR and PKC-θ are shown. In the *lower panels*, the percentages of KJ1.26$^+$ conjugates with polarized TCR or PKC-θ are shown. Thirty to 50 KJ1.26$^+$ conjugates were counted in each experiment. The results are shown as the average of four independent experiments ± SD. Values of p were calculated using the paired Student t test.

Ag-induced activation of Vav, Rac1, and cdc42 is defective in orally tolerized T cells

Next, we analyzed the biochemical basis underlying the defective translocation of TCR, PKC-θ, and lipid raft localization in orally tolerized T cells. Vav, a guanine nucleotide exchange factor for the Rho family GTPases Rac1 and cdc42, is a critical regulator for immunological synapse formation and raft recruitment to the synapse (48–51). Thus, we investigated tyrosine phosphorylation of Vav upon antigenic stimulation by Vav immunoprecipitation (Fig. 6*A*). Tyrosine phosphorylation of Vav was rapidly and significantly induced as early as 1 min upon antigenic stimulation in untreated control T cells. Phosphorylated Vav was seen 10 min after stimulation, although the levels were reduced. In sharp contrast, the levels of phosphorylation of Vav were not increased 1 min after stimulation in orally tolerized T cells. Interestingly, the levels of phosphorylation of Vav at 5 min were below those before stimulation. Phosphorylation of Vav was barely detectable 10 min after stimulation in these cells. We next investigated activation of Rac1 and cdc42 by the pull-down assay using GST-PAK-1 RBD, which specifically binds to Rac-GTP and cdc42-GTP (52). The GTP-bound, activated Rac1 and cdc42 were significantly induced upon antigenic stimulation in untreated control T cells (Fig. 6, *B* and *C*). Activation of Rac1 and cdc42 persisted for as long as 10 min. In contrast, activated Rac1 was not significantly induced beyond the levels before stimulation in orally tolerized T cells (Fig. 6*B*). Activated cdc42 was barely detectable upon antigenic stimulation in orally tolerized T cells (Fig. 6*C*). These differences in activation of Rac1 and cdc42 between untreated control and tolerized T cells were not due to differences in kinetics of activation because we did not observe increases in the levels of activated Rac1 and cdc42 at 15, 30, and 60 min after stimulation in orally tolerized T cells (data not shown). Taken together, our results indicate that defective activation of Vav/Rac1/cdc42 in orally tolerized T cells results in their defective translocation of TCR, PKC-θ, and lipid rafts into the interface between T cells and APCs

OVA-immunized T cells can form immunological synapses and activate vav, Rac, and cdc42

One may argue that any Ag-experienced T cells behave differently to naive T cells in terms of immunological synapse formation. Therefore, we finally made comparisons of orally tolerized T cells vs productively primed T cells. OVA-immunized T cells were prepared from spleen of DO11.10 mice immunized i.p. with OVA. Approximately 60–80% of these T cells showed phenotypes of

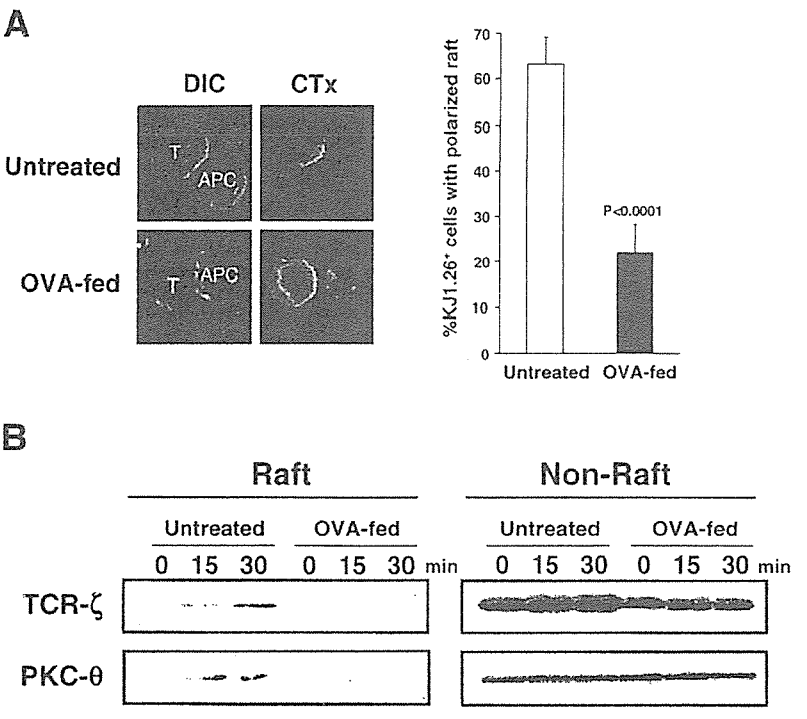

FIGURE 5. Ag-induced lipid raft translocation to the contact site and translocation of TCR and PKC-θ to lipid rafts in orally tolerized T cells. *A*, Splenic CD4 T cells were stained with FITC-CTx and then incubated with APCs prepulsed with 1 μM OVA323–339. After 30 min, cells were fixed and stained for KJ1.26$^+$TCR for confocal microscopy. In the *left panels*, representative images for T-APC conjugates and localization of the lipid rafts are shown. In the *right panels*, the percentages of KJ1.26$^+$ conjugates with polarized lipid rafts are shown. Thirty to 50 KJ1.26$^+$ conjugates were counted in each experiment. The results are shown as the average of four independent experiments ± SD. Value of p was calculated using the paired Student t test. *B*, Splenic CD4 T cells were incubated for the indicated times with APCs prepulsed with 50 μM OVA323–339. Cells were lysed in 1% Brij 98 lysis buffer. The lysates were subjected to ultracentrifugation, and 12 fractions were collected. Fractions 3 and 4 or fractions 10–12 were pooled as lipid raft fractions or nonraft fractions, respectively. The amounts of TCR-ζ and PKC-θ in lipid raft or nonraft fractions were analyzed by Western blotting. The results shown are representative of three independent experiments.

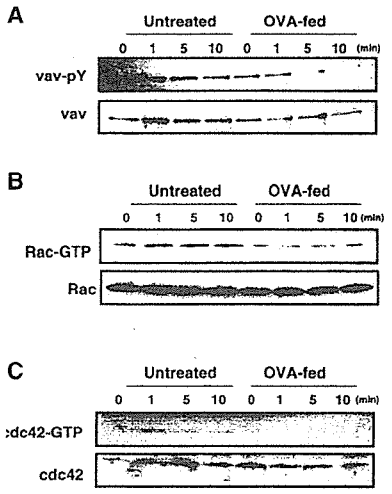

FIGURE 6. Activation of Vav, Rac1, and cdc42 in orally tolerized T cells upon antigenic stimulation. Splenic CD4 T cells were incubated for the indicated times with APCs prepulsed with 20 μM OVA323–339. *A*, Cells were lysed, and Vav was immunoprecipitated with anti-Vav Ab. The levels of tyrosine phosphorylation of Vav (*upper panel*) and total Vav (*lower panel*) were determined by Western blotting. *B*, Cells were lysed and active GTP-bound Rac was detected with a pull-down assay using GST-fusion PAK1-PBD. Bound Rac1 (*upper panel*) and total Rac1 (*lower panel*) were detected by Western blotting with anti-Rac1 Ab. *C*, Active GTP-bound cdc42 was detected as in *B*. Bound cdc42 (*upper panel*) and total cdc42 (*lower panel*) were detected with anti-cdc42 Ab.

memory/primed T cells as judged by CD62L and CD44 expression (data not shown). As shown in Fig. 7*A*, OVA-immunized T cells showed the same levels of proliferation and IL-2 production but greatly enhanced levels of IL-4 and IFN-γ production, compared with untreated control T cells, showing that these immunized T cells are productively primed to be differentiated to effector T cells.

No differences were seen in conjugate formation between immunized and orally tolerized T cells (Fig. 7*B*). However, in contrast to orally tolerized T cells, immunized T cells could accumulate TCR, PKC-θ, and lipid rafts at the interface between T cells and APCs. The frequencies of conjugates with polarized TCR, PKC-θ, and lipid rafts in immunized T cells were higher than those of untreated control T cells (Figs. 4 and 7*C*). As expected, in contrast to orally tolerized T cells, Ag-induced activation of vav, Rac1, and cdc42 was seen in immunized T cells (Fig. 7*D*). Thus, we conclude that impaired immunological synapse formation is specifically observed in orally tolerized T cells, not in any Ag-experienced T cells.

Discussion

In this article, we demonstrate that orally tolerized T cells can form stable conjugates with Ag-bearing APCs. However, these cells have defects in their translocation of TCR, PKC-θ, and lipid rafts to the interface between T cells and APCs. Biochemical analysis revealed intact activation of Rap1 but defective activation of Vav,

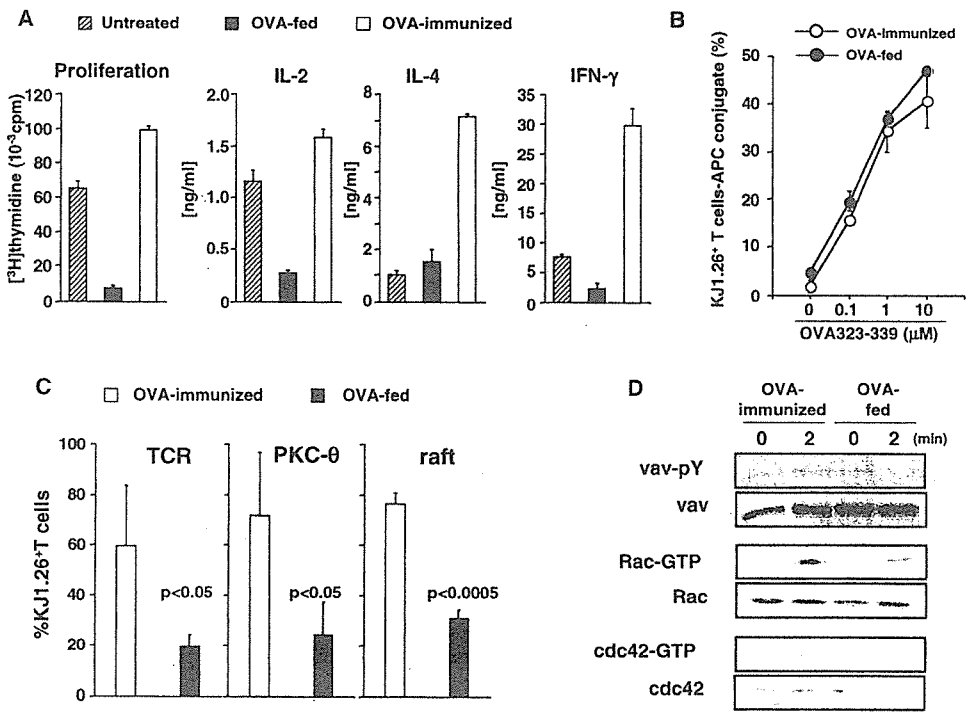

FIGURE 7. Conjugate formation, immunological synapse formation, and vav/Rac/cdc42 activation by T cells from OVA-immunized DO11.10 mice. *A*, Splenic CD4 T cells from untreated control (▨), OVA-fed (■), or OVA-immunized DO11.10 mice (□) were stimulated with 0.1 μM OVA323–339 in the presence of APCs. Proliferation between 48 and 72 h after stimulation was measured by [^{3}H]thymidine uptake. The culture supernatants were collected after 48 h, and concentration of IL-2, IL-4 and IFN-γ was determined by ELISA. The data are shown as the average of triplicate cultures ± SD. The results shown are representative of more than three independent experiments. *B*, Splenic CD4 T cells from OVA-immunized (○) or OVA-fed DO11.10 mice (●) were mixed with APCs prepulsed with indicated concentrations of OVA323–339. Conjugate formation after 30 min of incubation was determined as in Fig. 2. The data are shown as the average of triplicate cultures ± SD. The results shown are representative of three independent experiments. *C*, Splenic CD4 T cells from OVA-immunized (□) or OVA-fed DO11.10 mice (■) were incubated for 30 min with APCs prepulsed with 1 μM OVA323–339. The percentages of KJ1.26$^+$ conjugates with polarized TCR, PKC-θ, or lipid rafts were determined as in Fig. 4. The results are shown as average of three independent experiments ± SD. *D*, Splenic CD4 T cells from OVA-immunized or OVA-fed DO11.10 mice were incubated for 2 min with APCs prepulsed with 20 μM OVA323–339. Activation of vav, Rac1, and cdc42 was detected as in Fig. 6. The results shown as representative of three independent experiments.

Rac1, and cdc42 in orally tolerized T cells upon antigenic stimulation. These biochemical events induced by Ag stimulation correlate well with normal conjugate formation but impaired immunological synapse formation in orally tolerized T cells. The characteristics of TCR-mediated signaling in in vivo-tolerized T cells have been analyzed in various experimental systems (15–17). However, most of these studies used artificial, anti-TCR or anti-CD3 stimulation; therefore Ag-induced signaling, conjugate formation, and immunological synapse formation in in vivo-tolerized T cells have not been examined thus far. Therefore, this study provides new insight into Ag responsiveness of orally tolerized T cells. The findings are novel in that orally tolerized T cells are shown to form stable conjugates with APCs, without the accumulation of TCR, PKC-θ, and lipid rafts at the interface. The data suggest that not all functions are impaired in orally tolerized T cells. This is also supported by our biochemical data in that these T cells show normal activation of Rap1 (Fig. 3) and the Ras-ERK pathway (21). Furthermore, our data also suggests that conjugate formation and immunological synapse formation are regulated by distinct mechanisms. Thus, as seen in orally tolerized T cells, stable conjugate formation may not be always accompanied by immunological synapse formation.

Garcia et al. (53) have shown previously that hyporesponsive T cells from aged mice have defects in their immunological synapse formation. Their results are consistent with ours in that hyporesponsive T cells cannot translocate TCR or PKC-θ to the site of T-APC interaction. They also showed that various kinases, enzymes, and adaptors, such as lck, phospholipase C-γ (PLC-γ), linker for activation of T cells, Grb2, and Vav, are not accumulated in the contact site with APCs and T cells from aged mice. Recent work by Heissmeyer et al. (54) also demonstrated instability of the immunological synapse formation in in vitro-anergized T cells. These reports suggest that impaired immunological synapse formation could account for T cell hyporesponsiveness. In contrast, some differences were observed between our orally tolerized T cells and in vitro anergized T cells in terms of their immunological synapse formation. In vitro anergized T cells formed immunological synapses indistinguishable from those of normal T cells at early time points after incubation on lipid bilayers (54). However, the immunological synapse of anergized T cells was not stable and was broken down at later time points. We also analyzed the kinetics of accumulation of TCR and PKC-θ to the site of T-APC contact. However, we failed to observe translocation of these molecules in orally tolerized T cells at earlier time points (data not shown). The differences in synapse formation at early time points may be derived from the differences in the experimental systems, such as in vitro vs in vivo hyporesponsive T cells as responders, or lipid bilayers or live APCs as stimulators. It is important, anyhow, that in both studies, the majority of hyporesponsive T cells did not form proper immunological synapses at later time points because prolonged immunological synapse formation appears to be required for full T cell activation (29).

We demonstrated that translocation of lipid rafts to the contact site and TCR/PKC-θ recruitment to the lipid rafts is defective in orally tolerized T cells upon antigenic stimulation (Fig. 5). Lipid rafts are plasma membrane compartments enriched in key signaling molecules, such as lck, fyn, and linker for activation of T cells, and are thought to function as platforms in TCR signaling. Aggregation and translocation of lipid rafts is thought to stabilize the immunological synapse and result in sustained signaling leading to full activation (55). Thus, the failure of lipid raft clustering and translocation of signaling molecules into lipid rafts may result in defects in immunological synapse formation and affect downstream signaling events. It has been demonstrated that translocation of PKC-θ into lipid rafts and immunological synapse is required for NF-κB activation in T cells (28). Consistent with this, we have found that NF-κB nuclear translocation is defective in Ag-stimulated orally tolerized T cells (unpublished observation).

Orally tolerized T cells showed defective activation of Vav, Rac1, and cdc42 upon antigenic stimulation (Fig. 6). Knockout studies revealed that Vav is a critical regulator for rearrangement of the actin cytoskeleton, TCR capping, and cell adhesion (48, 51). Furthermore, it has been shown that lipid raft polarization into the immunological synapse depends on Vav/Rac function (50). Wiskott-Aldrich syndrome protein, a cdc42 effector, has also been shown to be required for TCR capping, lipid raft clustering, and immunological synapse formation (56). Taken together, defective activation of Vav/Rac1/cdc42 in orally tolerized T cells may be responsible for their impaired immunological synapse formation and raft translocation to the synapse.

The molecular basis underlying defective Vav activation in tolerized T cells remains unclear. However, we noted unique patterns of tyrosine phosphorylation of Vav observed in orally tolerized T cells upon antigenic stimulation (Fig. 6*A*). The levels of tyrosine phosphorylation of Vav 5 min after stimulation was below those of unstimulated T cells, although the levels of Vav protein were not changed. This may be explained by the idea that negative regulators for Vav are strongly activated upon stimulation and such molecules induce down-regulation of Vav phosphorylation in orally tolerized T cells. One of candidate negative regulator may be cbl-b, an E3 ubiquitin ligase (57, 58). Vav phosphorylation is strongly up-regulated in cbl-b$^{-/-}$ T cells upon TCR stimulation, suggesting that cbl-b is a negative regulator of Vav phosphorylation (59, 60). We found that cbl-b is highly expressed in orally tolerized T cells (data not shown). We are now investigating the mechanism of Ag-induced down-regulation of Vav phosphorylation in orally tolerized T cells, including the involvement of cbl-b activation.

We found that Rap1 activation remains intact in orally tolerized T cells upon antigenic stimulation (Fig. 3). Rap1 is a potent activator of integrins and is essential for LFA-1/ICAM-1-mediated interactions between T cells and APCs (41, 42). Inhibition of Rap1 activation by a dominant-negative Rap1 abrogates T-APC conjugate formation (41). Conversely, overexpression of Rap1 enhances conjugate formation (41). Thus, normal conjugate formation by orally tolerized T cells seems to be due to intact activation of Rap1.

Katagiri et al. (61) have demonstrated recently that Rap1 activation induced by TCR stimulation is dependent on PLC-γ and that Rap1activation is likely to be mediated by CalDAG-GEFI. In contrast, Amsen et al. (62) reported that Rap1 activation in thymocytes is induced in a PLC-γ-independent manner. The study also suggested that Cbl-C3G-CrkL may play an important role for Rap1 activation in thymocytes. We have demonstrated that PLC-γ is not activated in orally tolerized T cells upon TCR stimulation (21). Thus, it is likely that Rap1 activation in orally tolerized T cells is induced independently of PLC-γ pathways, as in the case of thymocytes.

It has been reported that human anergic T cell clones express active Rap1 constitutively (63) and that overexpression of constitutively active form of Rap1 inhibits IL-2 production by T cells by the down-regulation of Ras-ERK activation (63). The function of Rap1 as a negative regulator for T cell activation was confirmed by a knockout study of SPA-1, a principle Rap1 GTPase-activating protein, showing that accumulation of large amounts of active Rap1 correlated with T cell hyporesponsiveness and down-regulation of ERK activation (64). In our system, the levels of active Rap1 in orally tolerized T cells was higher, but only slightly, than those in control T cells (Fig. 3). Furthermore, Ras-ERK activation

induced by TCR stimulation was normal in orally tolerized T cells (21). Thus, it seems unlikely that Rap1 activation contributes to the hyporesponsiveness of orally tolerized T cells.

The biological meaning of normal conjugate formation by orally tolerized T cells is currently unknown. However, the formation of stable conjugates with APCs may help to regulate their own activation. It may be possible that stable and prolonged conjugate formation enables these T cells to elicit negative signaling, such as ubiquitin-mediated degradation of signaling proteins or phosphatase activation or to cause their own apoptosis. It has been demonstrated that orally tolerized T cells have immunoregulatory functions via the production of suppressive cytokines such as IL-10 or TGF-β (6, 65). Stable conjugate formation may be required to elicit such effector functions by tolerized T cells. These points should be clarified in future studies.

One may argue that regulatory T cells may play a role in our OVA-induced tolerance system. CD4 T cells from OVA-fed DO11.10 mice contained 15–30% of $CD25^+$ T cells (data not shown). Consistent with recent reports suggesting the suppressive function of $CD4CD25^+$ T cells in oral tolerance (66, 67), $CD4CD25^+$ T cells in OVA-fed DO11.10 mice were unresponsive to TCR stimulation but were able to inhibit naive T cell activation (data not shown). It is unknown whether these $CD4CD25^+$ T cells play some roles in induction of oral tolerance. However, depletion of the $CD4CD25^+$ T cells did not affect the proliferative response and IL-2 production by CD4 T cells from OVA-fed mice (data not shown), suggesting that the hyporesponsiveness of CD4 T cells in our system was not mediated by the $CD4CD25^+$ T cells. So far a few studies have addressed TCR-mediated signaling in naturally occurring $CD4CD25^+$ T cells (68, 69), but their characteristics concerning immunological synapse formation is still unknown. The comparison between anergic and $CD4CD25^+$ regulatory T cells in terms of their TCR-mediated signaling and immunological synapse formation should be performed.

In conclusion, this study demonstrates that orally tolerized T cells can form conjugates with APCs efficiently but fail to translocate TCR, PKC-θ, and lipid rafts to the contact site. This impairment of immunological synapse formation may be responsible for the hyporesponsive state of orally tolerized T cells. These findings will be helpful in providing a deeper understanding of the molecular mechanisms of peripheral tolerance.

Acknowledgments

We thank Drs. A. Kosugi, Y. Itoh, and K. Kimachi for their advice on lipid raft preparations, signaling assays, and conjugate formation assays, respectively.

Disclosures

The authors have no financial conflict of interest.

References

1. Mayer, L., and L. Shao. 2004. Therapeutic potential of oral tolerance. *Nat. Rev. Immunol.* 4: 407–419.
2. Melamed, D., and A. Friedman. 1993. Direct evidence for anergy in T lymphocytes tolerized by oral administration of ovalbumin. *Eur. J. Immunol.* 23: 935–942.
3. Migita, K., and A. Ochi. 1994. Induction of clonal anergy by oral administration of staphylococcal enterotoxin B. *Eur. J. Immunol.* 24: 2081–2086.
4. Van Houten, N., and S. F. Blake. 1996. Direct measurement of anergy of antigen-specific T cells following oral tolerance induction. *J. Immunol.* 157: 1337–1341.
5. Maloy, K. J., and F. Powrie. 2001. Regulatory T cells in the control of immune pathology. *Nat. Immunol.* 2: 816–822.
6. Chen, Y., V. K. Kuchroo, J. Inobe, D. A. Hafler, and H. L. Weiner. 1994. Regulatory T cell clones induced by oral tolerance: suppression of autoimmune encephalomyelitis. *Science* 265: 1237–1240.
7. Chen, Y., J. Inobe, R. Marks, P. Gonnella, V. K. Kuchroo, and H. L. Weiner. 1995. Peripheral deletion of antigen-reactive T cells in oral tolerance. [Published erratum appears in *1995 Nature* 377: 257.] *Nature* 376: 177–180.
8. Chen, Y., J. Inobe, and H. L. Weiner. 1995. Induction of oral tolerance to myelin basic protein in CD8-depleted mice: both $CD4^+$ and $CD8^+$ cells mediate active suppression. *J. Immunol.* 155: 910–916.
9. Linder, O., L. M. Santos, C. S. Lee, P. J. Higgins, and H. L. Weiner. 1989. Suppression of experimental autoimmune encephalomyelitis by oral administration of myelin basic protein. II. Suppression of diseases and in vitro immune responses is mediated by antigen-specific $CD8^+$ T lymphocytes. *J. Immunol.* 142: 748–752.
10. Ke, Y., K. Pearce, J. P. Lake, H. K. Ziegler, and J. A. Kapp. 1997. $\gamma\delta$ T lymphocytes regulate the induction and maintenance of oral tolerance. *J. Immunol.* 158: 3610–3618.
11. Fujihashi, K., T. Dohi, M. N. Kweon, J. R. McGhee, T. Koga, M. D. Cooper, S. Tonegawa, H. Kiyono, Y. Ke, J. P. Lake, H. K. Ziegler, and J. A. Kapp. 1999. $\gamma\delta$ T cells regulate mucosally induced tolerance in a dose-dependent fashion. *Int. Immunol.* 11: 1907–1916.
12. Garside. P. M., F. Y. Steel, and A. M. Mowat. 1995. $CD4^+$ but not $CD8^+$ T cells are required for the induction of oral tolerance. *Int. Immunol.* 7: 501–504.
13. Barone, K. S., S. L. Jain, and J. G. Michael. 1995. Effect of in vivo depletion of $CD4^+CD8^+$ cells on the inductin and maintenance of oral tolerance. *Cell. Immunol.* 163: 19–29.
14. Hirahara, K., T. Hisatsune, K. Nishijima, H. Kato, O. Shiho, and S. Kaminogawa. 1995. $CD4^+$ T cells anergized by high dose feeding establish oral tolerance to antibody responses when transferred in SCID and nude mice. *J. Immunol.* 154: 6238–6245.
15. Dubois, P. M., M. Pihlgren, M. Tomkowiak, M. Van Mechelen, and J. Marvel. 1998. Tolerant CD8 T cells induced by multiple injections of peptide antigen show impaired TCR signaling and altered proliferative responses in vitro and in vivo. *J. Immunol.* 161: 5260–5267.
16. Kimura, M., M. Yamashita, M. Kubo, M. Iwashima, C. Shimizu, K. Tokoyoda, J. Chiba, M. Taniguchi, M. Katsumata, and T. Nakayama. 2000. Impaired Ca/calcineurin pathway in in vivo anergized CD4 T cells. *Int. Immunol.* 12: 817–824.
17. Utting, O., S. J. Teh, and H. S. Teh. 2000. A population of in vivo anergized T cells with a lower activation threshold for the induction of CD25 exhibit differential requirements in mobilization of intracellular calcium and mitogen-activated protein kinase activation. *J. Immunol.* 164: 2881–2889.
18. Sundstedt, A., M. Sigvardsson, T. Leanderson, G. Hedlund, T. Kalland, and M. Dohlsten. 1996. In vivo anergized $CD4^+$ T cells express perturbed AP-1 and NF-κB transcription factors. *Proc. Natl. Acad. Sci. USA* 93: 979–984.
19. Sundstedt, A., and M. Dohlsten. 1998. In vivo anergized $CD4^+$ T cells have defective expression and function of the activating protein-1 transcription factor. *J. Immunol.* 161: 5930–5936.
20. Grundstrom, S., P. Anderson, P. Scheipers, and A. Sundstedt. 2004. Bcl-3 and NFκB p50–p50 homodimers act as transcriptional repressors in tolerant $CD4^+$ T cells. *J. Biol. Chem.* 279: 8460–8468.
21. Asai, K., S. Hachimura, M. Kimura, T. Toraya, M. Yamashita, T. Nakayama, and S. Kaminogawa. 2002. T cell hyporesponsiveness induced by oral administration of ovalbumin is associated with impaired NFAT nuclear translocation and p27kip1 degradation. *J. Immunol.* 169: 4723–4731.
22. Kaji, T., S. Hachimura, W. Ise, and S. Kaminogawa. 2003. Proteome analysis reveals caspase activation in hyporesponsive CD4 T lymphocytes induced in vivo by the oral administration of antigen. *J. Biol. Chem.* 278: 27836–27843.
23. Dustin, M. L., and J. A. Cooper. 2000. The immunological synapse and the actin cytoskeleton: molecular hardware for T cell signaling. *Nat. Immunol.* 1: 23–29.
24. Monks, C. R., B. A. Freiberg, H. Kupfer, N. Sciaky, and A. Kupfer. 1998. Three-dimensional segregation of supramolecular activation clusters in T cells. *Nature* 395: 82–86.
25. Grakoui, A., S. K. Bromley, C. Sumen, M. M. Davis, A. S. Shaw, P. M. Allen, and M. L. Dustin. 1999. The immunological synapse: a molecular machine controlling T cell activation. *Science* 285: 221–227.
26. Wulfing, C., and M. M. Davis. 1998. A receptor/cytoskeletal movement triggered by costimulation during T cell activation. *Science* 282: 2266–2269.
27. Viola, A., S. Schroeder, Y. Sakakibara, and A. Lanzavecchia. 1999. T lymphocyte costimulation mediated by reorganization of membrane microdomains. *Science* 283: 680–682.
28. Bi, K., Y. Tanaka, N. Coudronniere, K. Sugie, S. Hong, M. J. van Stipdonk, and A. Altman. 2001. Antigen-induced translocation of PKC-θ to membrane rafts is required for T cell activation. *Nat. Immunol.* 2: 556–563.
29. Huppa, J. B., M. Gleimer, C. Sumen, and M. M. Davis. 2003. Continuous T cell receptor signaling required for synapse maintenance and full effector potential. *Nat. Immunol.* 4: 749–755.
30. Balamuth, F., D. Leitenberg, J. Unternaehrer, I. Mellman, and K. Bottomly. 2001. Distinct patterns of membrane microdomain partitioning in Th1 and Th2 cells. *Immunity* 15: 729–738.
31. Kovacs, B., M. V. Maus, J. L. Riley, G. S. Derimanov, G. A. Koretzky, C. H. June, and T. H. Finkel. 2002. Human $CD8^+$ T cells do not require the polarization of lipid rafts for activation and proliferation. *Proc. Natl. Acad. Sci. USA* 99: 15006–15011.
32. Purbhoo, M. A., D. J. Irvine, J. B. Huppa, and M. M. Davis. 2004. T cell killing does not require the formation of a stable mature immunological synapse. [Published erratum appears in *2004 Nat. Immunol.* 5: 658.] *Nat. Immunol.* 5: 524–530.
33. Ardouin, L., M. Bracke, A. Mathiot, S. N. Pagakis, T. Norton, N. Hogg, and V. L. Tybulewicz. 2003. Vav1 transduces TCR signals required for LFA-1 function and cell polarization at the immunological synapse. *Eur. J. Immunol.* 33: 790–797.
34. Richie, L. I., P. J. Ebert, L. C. Wu, M. F. Krummel, J. J. Owen, and M. M. Davis. 2002. Imaging synapse formation during thymocyte selection: inability of CD3ζ